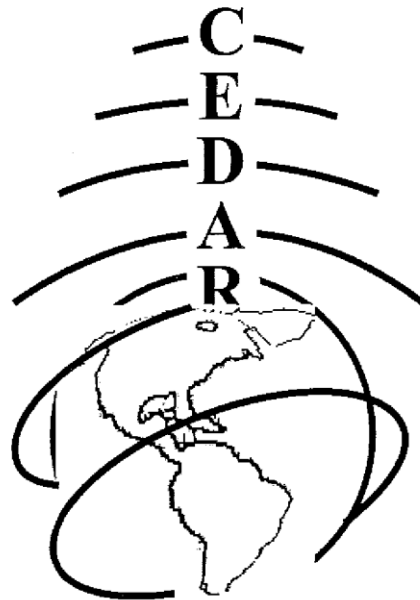




2009 CEDAR Workshop
Eldorado Hotel
Santa Fe, New Mexico, USA
June 28 – July 2, 2009



Tuesday CEDAR Poster Session Booklet
June 30, 2009



Table of Contents

Solar Terrestrial Interactions in the Upper Atmosphere

SOLA-01, Kelly Ann Drake, High-latitude Poynting flux observations during the solar and geomagnetic activity in September 2005.....	1
SOLA-02, David Gerhardt, Colorado Student Space Weather Experiment (CSSWE): In-situ Measurements of Solar Energetic Particles.....	1
SOLA-03, Barbara Emery, Solar Forcing of Electron and Ion Auroral Inputs	1
SOLA-04, Yvonne Rinne, Stratification of newly reconnected flux in the polar cap ionosphere.....	2
SOLA-05, David Pawlowski, An investigation into the effect of solar flares on the thermosphere	2
SOLA-06, Mariangel Fedrizzi, Variability and climatology of the upper atmosphere during IPY using CTIPe physical-model	3
SOLA-07, Ellen Pettigrew, A Statistical Model of Ionospheric Convection in the Southern Hemisphere.....	3
SOLA-08, Delores Knipp, Enhanced Thermospheric Density: The Roles of In-the-Ecliptic and Northward Interplanetary Magnetic Field	3
SOLA-09, Chin Lin, Occurrence of High Latitude Neutral Density Peaks	4
SOLA-10, Katherine Roach, Variation of the Vertical Thermospheric Wind Gradients	4
SOLA-11, Xiaoli Luan, Seasonal and hemispheric variations of the total auroral precipitation energy flux from TIMED/GUVI.....	4
SOLA-12, Justin Yonker, Fluorescence of the N2 Birge-Hopfield I System in the Thermospheric Dayglow	5
SOLA-13, Tomoko Matsuo, Principal modes of thermospheric density variability: empirical orthogonal function analysis of CHAMP 2001-2008 data.....	5
SOLA-14, Xianjing Liu, Altitude dependence of the thermospheric density response to the solar and geomagnetic forcing.....	5
SOLA-15, Yong Shi, Tail and ionospheric signatures of tail fast flows associated with PBIs and with Substorms, presented by Larry Lyons	6
SOLA-16, Russell Stoneback, Effective Aperture Behavior of Open Magnetic Field Lines in the Geospace Environment and on the Sun	6
SOLA-17, Serge Minin, Fabry-Perot measurements of H-alpha emissions at Arecibo observatory during geomagnetic Storms	7

Instruments or Techniques for Ionospheric or Thermospheric Observation

ITIT-01, Serge Minin, Uncertainties in extracted Gaussian emission line parameters: measurement setup choices in Doppler spectroscopy with continuum background	7
ITIT-02, Alexander Hackett, Multi-purpose Radar Controller.....	7
ITIT-03, Benjamin Burnett, Statistical analysis of high-latitude F-region ionospheric composition.....	7
ITIT-04, Gary Bust, Validation of IDA4D estimates of F-region electron densities using CHAMP in-situ and ground-based ionosonde observations of electron density	8
ITIT-05, Eli Hibit, Numerical Predictions on Mid-Latitude Ionospheric Locations	8
ITIT-06, Hugh Gallagher, The NorthEast CIDR Array: A new chain of ionospheric tomography receivers for studying the equatorward edge of the auroral oval and the mid-latitude trough, presented by Allen Weatherwax.....	8
ITIT-07, Trevor Garner, An Auroral Scintillation Observation using Precise Collocated GPS Receivers.....	9
ITIT-08, Ayman us, The First Result of Coherent Ionospheric Doppler Receiver Measurements over Egypt, presented by Trevor Garner.....	9
ITIT-09, Stephen Bayne, Observations of the auroral electrojet plasma using UHF/VHF radio beacon measurements	9
ITIT-10, Ryan Davidson, Development, Simulations, and Validations of CubeSat Retarding Potential Analyzer	10
ITIT-11, Konstantinos Kalogerakis, Remote Oxygen Sensing by Ionospheric Excitation (ROSIE)	10
ITIT-12, Patrick Roddy, Initial Electron Temperature Results from the Planar Langmuir Probe on C/NOFS.....	10
ITIT-13, Lei Zhang, Robust GPS Signal Tracking Under Ionosphere Scintillation.....	10
ITIT-14, Cesar De La Jara, The LISN database: Description and initial results	11
ITIT-15, Brady O'Hanlon, First Observations of Equatorial TEC and Scintillation with Multiple Dual-Frequency Software-Defined GPS Receivers.....	11
ITIT-16, Jeffrey Spaleta, Application of Bayesian Spectral Analysis to SuperDARN ACF Data.....	11
ITIT-17, Richard Todd Parris, Imaging with the Kodiak Island SuperDARN HF Radar	12

ITIT-18, Rabiano Rodrigues, Simultaneous radar measurements of daytime zonal and vertical plasma drifts in Peru and Brazil.....	12
ITIT-19, Fabiano Rodrigues, An alternative approach for estimating E-region density profiles from GPS radio occultation measurements	12
ITIT-20, Romina Kiloukar, Amplitude modulation for Arecibo F-region ISR experiments.....	13
ITIT-21, Marcin Pilinski, Understanding Biases in Atmospheric Density Derived from Satellite Drag	13
ITIT-22, Steven Burr, Advanced techniques of tomographic reconstruction algorithms for observing the night time ionospheric air glow	14
ITIT-23, Andres Stephan, RAIDS: A New Mission for Ionospheric and Lower Thermospheric Science.....	14
ITIT-24, Matthew Sunderland, Design of a Digital Pulsed Radar Receiver: Increasing Aeronomy Observation Bandwidth at Arecibo Observatory	14
ITIT-25, Sandeep Anna Kor, Optimization of GC314 Digital Receiver.....	15
ITIT-26, Padmashri Suresh, Estimation of Langmuir Probe Currents in the event of Surface Potential Variation	15
ITIT-27, Siming Zhao, The role of geomagnetic field on the occurrence of specular meteor trails.....	15
ITIT-28, Christopher Watts, Ionospheric measurements from LWA calibration.....	16
ITIT-29, Yiyi Huang, Estimation of Temperature and Wind Velocity Profiles in Upper Atmosphere Using Fabry-Perot Interferometers	16
ITIT-30, Priyanka Chandrasekran, Higher Order Ionosphere Error in GPS Measurements, presented by Yu Morton	16

Data Assimilation

DATA-01, Nick Matteo, Ionosphere geomagnetic field: comparison of IGRF model prediction and satellite measurements, presented by Yu Morton.....	16
DATA-02, Donald Rice, An Expert System for Ionogram Reduction (ESIR).....	17
DATA-03, Juan Urco Cordero, The Madrigal database at Jicamarca Radio Observatory: Data from the main instruments of Jicamarca available to the world	17
DATA-04, Akinori Saito, Dagik: Data-showcase system for the geospace using Google Earth, presented by Michi Nishioka.....	18

Equatorial Ionosphere or Thermosphere

EQIT-01, Michi Nishioka, Preliminary Comparison of In-Situ Plasma Density Structures from C/NOFS at dusk wit TEC and Scintillation Data from LISN obtained during October 2008	18
EQIT-02, Glenn Joyce, Atomic and molecular ion dynamics during equatorial spread F.....	18
EQIT-03, Jonathan Krall, Three-Dimensional Modeling of Equatorial Spread-F Airglow Enhancements	19
EQIT-04, Narayan Chapagain, Ionospheric OI 630 nm Airglow Depletion Zonal Velocities over Ascension Island.....	19
EQIT-05, Ronald Ilma, On the possibility to infer ionospheric electric fields from the bottomside equatorial F-region Irregularities	19
EQIT-06, Yi-Jiun Su, Assimilative Modeling of Equatorial Plasma Depletions Observed by C/NOFS	20
EQIT-07, Yann Paul Tambouret, Investigating Medium to Short Scale E-region Gradient Drift Waves Using Hybrid Simulations.....	20
EQIT-08, Ethan Miller, Equatorial Spread-F in the Central Pacific: Seven Years of Airglow and Radar Data	20
EQIT-09, Ehtan Miller, Coincidence of Equatorial and Mid-Latitude Irregularities	21
EQIT-10, Gopi Kreshna Seemala, Studies of equatorial spread F using LISN VIPIR.....	21
EQIT-11, Tzu-Wei Fang, Causal link of the wave-4 structures in plasma density and vertical plasma drift in the low-latitude ionosphere	21
EQIT-12, Joe McInerney, The Thermospheric Midnight Temperature Maximum (MTM) As Seen in the Extended Whole Atmosphere Community Climate Model (WACCM-X).....	22
EQIT-13, Robert Haaser, C/NOFS Neutral Wind Meter Measurements of Neutral Thermospheric Helium Dominance at 400 km during Extreme Solar Minimum.....	22
EQIT-14, Patrick Alken, Modeling the day-time eastward equatorial electric field	22
EQIT-15, Christopher Miller, Use of Incoherent Scatter Radar Data to Study the Equatorial Midnight Temperature Maximum (MTM)	23
EQIT-16, John Meriwether, The detection of a secondary peak in the nighttime measurements of thermospheric temperatures at Arequipa Peru (16.5S, 71.5 W).....	23

EQIT-17, Nicholas Pedatell, Inter-annual variability in the longitudinal structure of the low-latitude ionosphere due to the El-Nino Southern Oscillation	23
EQIT-18, Michael Olson, Equatorial Zonal Electric Fields during the 2003 Sudden Stratospheric Warming Event	24
EQIT-19, Pablo Reyes, Estimation of ionospheric temperatures using Jicamarca IS radar data with beams pointed perpendicular to the geomagnetic field	24
EQIT-20, Seebany Datta-Burua, Estimating Model Parameters from Ionospheric Reverse Engineering	24
EQIT-21, Glenn Sugar, Non-specular meteor measurements of lower thermosphere winds	25

Long-Term Variations of the Upper Atmosphere

LTRV-01, Susan Nossal, Long Term Monitoring of Geocoronal Hydrogen	25
LTRV-02, Eva Robles, Climatology of the antiparallel plasma drift over Arecibo Observatory	26

Midlatitude Ionosphere or Thermosphere

MDIT-01, Diana Prado, Topside ionosphere responses to a moderate geomagnetic storm	26
MDIT-02, Yun Gong, Numerical simulation and observational study of ion layer formation at Arecibo	26
MDIT-03, Edgardo Pacheco, Quiet time Latitudinal Variations of Ion drifts in the Ionosphere at Low-and Middle Latitudes	26
MDIT-04, Edvier Cabassa-Miranda, Analysis of Arecibo dual beam world day data from 2006 to present – Results from the weakest solar minimum since 1928	27
MDIT-05, Larisa Goncharenko, Ionospheric variations during January 2009 stratospheric sudden warming	27
MDIT-06, Larisa Goncharenko, Joint FPI/ISR Observations at Millstone Hill Observatory	27
MDIT-07, Peichen Lai, COSMIC Observations of TEC Enhancements during Magnetic Disturbances	28
MDIT-08, Ilgin Seker, The Properties and 3D Structure of Medium Scale Traveling Ionospheric Disturbances	28
MDIT-09, Tatsuhiro Tokoyame, Three-dimensional simulation of the coupled Perkins and Es layer instabilities in the night time midlatitude ionosphere	29
MDIT-10, Jonathan Thompson, Tool for the Assessment of Ionospheric Models	29
MDIT-11, Gregory Twork, Midlatitude Observations of the Thermosphere Implementing a Fabry-Pérot Interferometer ...	29
MDIT-12, Russell Hedden, SOFDI/CASI Observations of the September 2005 Storm	30
MDIT-13, Elise Larson, Multi Line Investigations of the Hydrogen Geocorona, presented by Edwin Mierkiewicz	30
MDIT-14, Goderdzi Didebulidze, Impulse-like increase of the nightglow [OI] 630 nm line intensity and its possible reason as a shear excited atmospheric vortical perturbations, presented by Nikoloz Gudaze	30
MDIT-15, Yan Yin, Prompt Penetration of the Interplanetary Electric Field to the Mid Latitude Ionosphere	31

Polar Aeronomy

POLA-01, Erik Lundberg, Preliminary Results from the CASCADES-2 Sounding Rocket	31
POLA-02, Matthew Zettergren, Dynamic variability in ionospheric composition at high latitudes	31
POLA-03, Carl Andersen, Measurement of E-region neutral winds with the Poker Flat all-sky imaging Fabry-Perot Spectrometer	32
POLA-04, Thomas Butler, Estimation of vector velocity field using an array of spatially distributed ISR measurements ...	32
POLA-05, Gabriel Michhue, The role of k_{\parallel} on wave heating in the auroral E region	32
POLA-06, Brent Sadler, Numerical Estimates of Polar Cusp Neutral Upwelling Using Satellite Conjunction Data	33
POLA-07, Erik Stromberg, Double Probe Electric Field Measurements	33

Solar Terrestrial Interactions in the Upper Atmosphere

SOLA-01 High-latitude Poynting flux observations during the solar and geomagnetic activity in September 2005 - by Kelly Ann Drake

Status of First Author: Non-student

Authors: K. A. Drake, USAF Academy, D. J. Knipp, HAO, NCAR, G. Crowley, ASTRA

Abstract: A major goal of solar-terrestrial physics is to improve the understanding of the coupled solar wind – magnetosphere – ionosphere – thermosphere (SW-M-I-T) system. Energy input to the Earth’s atmosphere due to the interaction between the solar wind and the magnetosphere occurs primarily at high latitudes. Poynting’s theorem provides a general description of electromagnetic energy exchange between the magnetosphere and upper atmosphere. In September 2005, a series of complex solar events and multiple shocks were observed by GOES and SOHO. Geomagnetic conditions were influenced by the arrival of five halo CMEs recorded from the 7th to the 13th. Using in-situ ion drift and magnetometer measurements from DMSP F15 during these events, high-latitude Poynting flux is calculated and compared to solar wind parameters (e.g. solar wind speed, pressure, temperature, density, and IMF direction) measured by the ACE satellite, geomagnetic activity (e.g. SymH), and thermospheric density response measured by the CHAMP satellite. Rapid and large increases and decreases in the solar wind dynamic pressure, large increases in the solar wind velocity (high-speed streams), and other solar wind drivers, produce changes in the coupling efficiency. Correlating measurements from diverse locations and satellites during these unusual and not well-modeled events expands our understanding of energy deposition from SW-M-I-T coupling.

SOLA-02 Colorado Student Space Weather Experiment (CSSWE): In-situ Measurements of Solar Energetic Particles - by David Gerhardt

Status of First Author: Student IN poster competition PhD

Authors: David Gerhardt, Drew Turner, Tyler Redick, Jianbao Tao.

Abstract: Solar Energetic Particles (SEPs) are high-energy electrons and protons resultant of solar flares or coronal mass ejections. These particles can pose a serious hazard to spacecraft and life in space; they are also important to upper atmospheric dynamics. The Colorado Student Space Weather Experiment (CSSWE) aims to develop a 3U CubeSat which includes an electron/proton telescope capable measuring the energy of SEPs. This telescope, the Relativistic Electron and Proton integrated little experiment (REPTile), is a miniaturization of a telescope previously employed by the Laboratory for Atmospheric and Space Physics (LASP). The energy measurements are validated by a complex statistical model of particle interactions with the surfaces of the instrument. The satellite employs passive magnetic attitude to maintain pointing along the magnetic field lines of Earth, maximizing particle flux to REPTile while minimizing mass and power.

SOLA-03 Solar Forcing of Electron and Ion Auroral Inputs - by Barbara Emery

Status of First Author: Non-student

Authors: Barbara A. Emery (NCAR, emery@ucar.edu), Ian G. Richardson (GSFC), David S. Evans (NOAA), Frederick J. Rich (LL/MIT), Gordon Wilson (AFRL), Sarah Gibson (NCAR), Giuliana deToma (NCAR), and Terry Onsager (NOAA)

Abstract: We assess the contribution of solar forcing from the interplanetary magnetic field (IMF) and solar wind velocity (V_{sw}) on the auroral inputs. The auroral total (HPt) or electron hemispheric power (HPe) is calculated from 1978 using intercalibrated NOAA and DMSP satellite-track in-situ particle measurements up to 20 keV, while the auroral ion hemispheric power (HPi) is calculated from the NOAA satellites since 1982 as the difference between the total and electron only HP (HPi=HPt-HPe). Hourly global auroral inputs of the electron (Pe) and ion power (Pi) are found as the sum of HP estimated in both hemispheres. Cross-correlations and fits are made between the auroral inputs and solar parameters. Periodicities in the hourly V_{sw} , IMF, Pe and Pi are calculated using Lomb-Scargle (L-S) on a yearly or longer basis for the entire period of observations. Pe and Pi exhibit solar rotational periodicities similar to those for V_{sw} , where the 9-day periodicity is particularly strong in 2005-2008, and is present also in the Kp index, in neutral densities ~400 km, and in infrared cooling by [NO] and [CO₂] between 100-200 km. This 9-d periodicity is not found in solar UV radiation or the

10.7 cm solar flux. The effects of different solar wind structures (transients (CMEs), high-speed streams (HSS) and slow-speed wind are also investigated.

We examine two different solar minimum periods in a broader context, including radiation belt electrons >2 MeV. The first Whole Sun Month (WSM) interval (96223-96252) had a strong solar magnetic dipole. A strong 'semiannual' periodicity of $\sim 20\%$ variation in V_{sw} maximizing in equinoxes was found, which enhanced the equinoctial maxima found in P_e (and K_p) due to the preferred solar wind and magnetospheric reconnection during equinoxes. Equinoctial peaks in V_{sw} at 1 AU are possible because the Earth's orbit reaches the highest solar latitudes ($+7.2$ deg) on 6 March and lowest (-7.2 deg) on 6 September. The average equinoctial variation is an increase of $\sim 15\%$ in P_e in equinoxes compared to solstices, but the equinoctial increase in 1996 of P_e was $\sim 40\%$. In the present solar minimum, the solar magnetic field is weaker with larger quadrupole components during the Whole Heliospheric Interval (WHI, 08080-08107). No semiannual periodicity was found in the auroral inputs or K_p , but a very strong 9-d amplitude of $\sim 40\%$ variation was found in P_e and P_i , which was related to a 9-d amplitude of $\sim 30\%$ variation in V_{sw} . This 9-d periodicity was also found in the outer radiation belt electrons >2 MeV. The radiation belt electrons were low in 1996 and elevated in 2008, possibly because of the 35% drop in the solar wind density which may control the loss processes.

SOLA-04 Stratification of newly reconnected flux in the polar cap ionosphere - by Yvonne Rinne

Status of First Author: Student IN poster competition PhD

Authors: Y. Rinne (1,2), J. Moen (1,2), H.C. Carlson (1,3)

1Department of Physics, University of Oslo, Oslo, Norway

2Arctic Geophysics, The University Centre in Svalbard, Svalbard, Norway

3Air Force Research Laboratory, EOARD, London, UK

Abstract: Using the European Incoherent Scatter (EISCAT) Svalbard Radar we obtained high resolution mapping of individual ionospheric plasma flow channels in clear response to sudden recurring rotations of the IMF. Three negative excursions of the IMF B_y component resulted in a train of eastward directed flow channels intermitted by periods of westward flow propagating into the polar cap. Hence, subsequent FTE flow channels stay in stark contrast to each other.

The negative excursions of the IMF B_y component are accompanied by positive excursions of the IMF B_z component shifting the active region favored for reconnection between low- and high latitude magnetopause.

The high spatial and temporal resolution of the data from the EISCAT Svalbard Radar enables us to track formation and movement of the channels, and hence observe how a newly reconnected flux stratifies in the ionosphere and propagates into the polar cap.

Our observations do not seem to support the Southwood (1987) model but are principally consistent with a picture by Lockwood (2001).

Southwood, D.J., The Ionospheric Signature of Flux Transfer Events. *J. Geophys. Res.* 92 (A4), 3207-3213 (1987)

Lockwood, M. et al., Cusp ion steps, field-aligned currents and poleward moving auroral forms. *J. Geophys. Res.* 106 (A12), 29,555-529,569 (2001)

SOLA-05 An investigation into the effect of solar flares on the thermosphere - by David Pawlowski

Status of First Author: Student IN poster competition PhD

Authors: David J. Pawlowski, dpawlows@umich.edu, Aaron J. Ridley, Atmospheric, Oceanic and Space Sciences, University of Michigan, Ann Arbor, MI

Abstract: Knowledge of the state of the Earth's upper atmosphere is extremely important for operational reasons, one of which being that perturbations in density and temperature can have a significant effect on low-Earth orbiting spacecraft. Since the ionosphere-thermosphere system is primarily determined by external forcing, there is a great deal of interest in understanding how the upper atmosphere responds to the transient features in the space environment. Observations have

shown, though, that the state of the thermosphere prior to a transient event can have an effect on the response to external dynamics. In this study, the Global Ion-osphere-Thermosphere Model (GITM) is used to investigate how the characteristics of solar flares, as well as the background state of the atmosphere, affect the thermospheric response to flares.

SOLA-06 Variability and climatology of the upper atmosphere during IPY using CTIpe physical-model
- by Mariangel Fedrizzi

Status of First Author: Non-student

Authors: Fedrizzi, M., Codrescu, M. V., Dobbin, A. L., Fuller-Rowell, T. J.

Abstract: The International Polar Year (IPY) has made quality high-latitude ionospheric data available in unprecedented quantities. The existence of a year-long continuous high-latitude data base of incoherent scatter radar (ISR) observations of the ionosphere provides an unprecedented opportunity for model/data comparisons. In the past, physics-based ionospheric models have usually only been compared with observations over restricted one or two day events or against climatological averages. In this study, using ISR ionospheric observations and CHAMP satellite neutral density measurements, the daily space weather, day-to-day variability, and year-long climatology of the three-dimensional, time-dependent, physics-based Coupled Thermosphere Ionosphere Plasmasphere Electrodynamics (CTIpe) model have been simultaneously addressed to identify modeling shortcomings and successes.

SOLA-07 A Statistical Model of Ionospheric Convection in the Southern Hemisphere - by Ellen Pettigrew

Status of First Author: Student IN poster competition Masters

Authors: Ellen Pettigrew (pettigrew@dartmouth.edu), Dartmouth College, Simon Shepherd, Dartmouth College, J. Mike Ruohoniemi, Virginia Tech

Abstract: In the past, data from the SuperDARN coherent scatter radars has been used to develop a statistical model of high latitude convection in the northern hemisphere ionospheric, dependent on interplanetary magnetic field (IMF) conditions. These “average” convection patterns are used both as a climatological model of the convection electric field in the ionosphere and in calculating instantaneous convection patterns from real-time SuperDARN data. Until now, however, no such statistical model existed for the southern hemisphere ionosphere. We have reproduced the model of northern hemisphere convection and have developed for the first time a corresponding model of southern hemisphere convection. Comparing these models enables us to highlight inter-hemispheric symmetries and asymmetries. Furthermore, since these models have been found to underestimate the instantaneous convection electric field, we are also studying the effect of including a solar wind velocity dependence in the model, giving a potentially more accurate estimation of the coupling strength.

SOLA-08 Enhanced Thermospheric Density: The Roles of In-the-Ecliptic and Northward Interplanetary Magnetic Field - by Delores Knipp

Status of First Author: Non-student

Authors: D. J. Knipp, HAO, NCAR, K. A. Drake, USAF Academy. J. Lei, University of Colorado, Boulder, G. Crowley, ASTRA

Abstract: During 2005 solar EUV energy input to the thermosphere waned as Solar Cycle 23 declined. The reduction allowed a clearer delineation of episodic thermospheric density disturbances caused by geomagnetic storms. We show new views of these disturbances based on Poynting flux calculations from the Defense Meteorological Satellite Program (DMSP) F-series satellites, as well as from accelerometer data from polar orbiting satellites, and from the Thermospheric Ionospheric Electrodynamics General Circulation Model (TIEGCM).

The new Poynting flux estimates allow us to trace the origins of disturbances that are poorly specified by ground indices. In particular we find that intervals of enhanced northward Interplanetary Magnetic Field (IMF) may allow significant electromagnetic energy input into localized regions of the high-latitude thermosphere. This energy deposition is consistent with IMF-geomagnetic field merging tailward of the Earth’s magnetic cusps. Energy access is likely controlled by Earth’s

dipole tilt. Of particular interest is the likelihood that this energy is not well captured or characterized by ground based indices.

We illustrate the results of this type of energy input with case-studies of events arriving at Earth between May and September 2005. We illustrate examples of the influence of high-speed streams and solar wind shock events that result in thermospheric density variations that themselves may be precursors to traveling atmospheric disturbances.

SOLA-09 Occurrence of High Latitude Neutral Density Peaks - by Chin S Lin

Status of First Author: Non-student

Authors: Chin S. Lin, AFRL, chin.lin@us.af.mil, Cheng-Yung Huang, Boston College, Frank A. Marcos, AFRL

Abstract: The occurrence distribution of large high latitude (> 60) neutral density peaks at 400 km associated with solar wind electric and magnetic field pulses was examined using CHAMP accelerometer data during the four and a half year period from mid-2001 through 2005. Peaks of the total mass density were generally detected around the dayside cusp between 09 and 16 MLT, suggesting the persistent presence of a density enhancement cell structure in this region. In addition many density peaks were detected inside the polar cap with > 70 magnetic latitude from 22 to 09 MLT during periods of moderate geomagnetic activity. There is a general correlation between occurrence of peaks and sudden enhancements of the Interplanetary magnetic and electric fields. NCAR's Thermosphere Ionosphere Electrodynamics Global Circulation Model (TIEGCM) was run for this event using the ACE interplanetary parameters. The overall temporal variation of high latitude neutral density in the TIEGCM modeling is similar to the CHAMP observation. TIEGCM modeling shows enhancement of neutral density in a broad region near the dayside cusp, but no enhancement near where CHAMP detected the density peak.

SOLA-10 Variation of the Vertical Thermospheric Wind Gradients - by Katherine Roach

Status of First Author: Student IN poster competition PhD

Authors: K.A. Roach (1), D.P. Drob (1), G. Crowley (2), A.G. Burns (3) S.E. McDonald (1)
(1) Space Science Division, US Naval Research Laboratory, 4555 Overlook Ave. SW, Washington, DC
(2) Atmospheric and Space Technology Research Assoc. (ASTRA), 11118 Quail Pass, San Antonio, TX
(3) High Altitude Observatory, National Center for Atmospheric Research, Boulder, Colorado

Abstract: Comparisons of the Horizontal Wind Model (HWM07) to a first-principles physics model (TIME-GCM) have shown that HWM07 does not model the vertical gradients seen in the TIME-GCM upper thermospheric winds during solar maximum. These gradients are caused by increased solar irradiance which increases the amount of ion drag in the thermosphere, the effect of which can dominate over the molecular viscosity that usually smoothes out these vertical gradients. The large gradients are missing in the HWM07 output since the model does not take the solar cycle into account. In order to add a solar cycle dependence to HWM07, we attempt to quantify the dependence of the vertical gradients on F107 by examining TIME-GCM output as a function of F107 and by looking at TIE-GCM output for simulations run at a constant F107.

SOLA-11 Seasonal and hemispheric variations of the total auroral precipitation energy flux from TIMED/GUVI - by Xiaoli Luan

Status of First Author: Non-student

Authors: Xiaoli Luan, Wenbin Wang, Alan Burns, and Stanley Solomon, High Altitude Observatory, National Center for Atmospheric Research, Boulder, CO, USA (luanxl@ucar.edu), Yongliang Zhang and Larry J. Paxton, Applied Physics Lab, Johns Hopkins University, MD, USA

Abstract: Abstract: The seasonal and hemispheric variations of Hemispheric Power (HP) of auroral precipitation are investigated under different geomagnetic conditions. The hemispheric power, which is the total auroral electron precipitation energy flux over the auroral oval area in one hemisphere, is calculated from the averaged energy flux derived from Far-ultraviolet emissions of the Global Ultraviolet Imager (GUVI) instrument on board the TIMED satellite. Using

observation from 2002 to 2007, the seasonal variations of the hemispheric power are separated from its hemispheric dependence. The results show that there is almost no June/Southern winter to December/Northern winter difference under all conditions. On the other hand, under geomagnetically quiet conditions ($K_p \leq 3$), the hemispheric power presents significant summer-winter and June/Northern summer to December/Southern summer differences, which vary between 5%-35% and decrease with increase of the K_p index. These seasonal variations of the hemispheric power disappear under geomagnetically disturbed conditions ($K_p = 4, 5$).

SOLA-12 Fluorescence of the N₂ Birge-Hopfield I System in the Thermospheric Dayglow
by Justin David Yonker

Status of First Author: Student IN poster competition PhD

Authors: Justin D. Yonker, Scott M. Bailey

Abstract: Excitation of the N₂ Birge-Hopfield I (b-X) system in the thermosphere is one of the major extinction mechanisms of solar irradiance below 100 nm. Because the absorption cross-section is so large, the optical depth of the b-x system increases faster with decreasing altitude than most any other dayglow system. Understanding the b state is thus key to a proper knowledge of the altitude deposition of the irradiance.

The b state may also be excited by collisions with photoelectrons produced by the solar irradiance shortward of 50 nm. While most of the b state vibrational levels are dissociated, fluorescence has been observed from the b(v'=1) level with the yield showing a sensitive dependence on rotational level. In this presentation, the significance of the different selection rules governing the two excitation processes is explored and the b-X fluorescence is modelled using recent determinations of the oscillator strengths and line widths. Comparison of the model with an observed dayglow spectrum from the Far Ultraviolet Spectroscopic Explorer (FUSE) will thus provide a gauge of our understanding of the extinction of the solar irradiance.

SOLA-13 Principal modes of thermospheric density variability: empirical orthogonal function analysis of CHAMP 2001-2008 data - by Tomoko Matsuo

Status of First Author: Non-student

Authors: Tomoko Matsuo, Cooperative Institute for Research in Environmental Sciences, University of Colorado, Boulder, Colorado, Jeffrey M. Forbes, Department of Aerospace Engineering Sciences, University of Colorado, Boulder, Colorado

Abstract: In this paper we characterize the dominant modes of global density variability as empirical orthogonal functions (EOFs) using densities obtained from the accelerometer experiment on board the CHAMP satellite during 2001-2008. We determine the significance of different types of thermospheric density variability to the overall density variation and also the importance of various external drivers of these primary modes of variability. From a sequential non-linear regression analysis of the density observations along satellite trajectories, we obtain EOFs in latitude/local-time coordinates and their orbit-time dependent amplitudes.

EOF1 includes a strong global mean component and takes the form of the diurnal variation. It correlates highly with the daily F10.7 index. EOF2 has a hemispherically asymmetric structure, and represents the summer-to-winter annual density variation. Density responses to geomagnetic forcing are primarily manifested in two different modes: EOF1 that represents the global mean response and EOF4 whose main features are high-latitude density increases.

SOLA-14 Altitude dependence of the thermospheric density response to the solar and geomagnetic forcing - by Xianjing Liu

Status of First Author: Student NOT in poster competition PhD

Authors: Xianjing Liu, xianjing@colorado.edu, Jeffrey P Thayer, jeffrey.thayer@colorado.edu, Jiuhou Lei, Jiuhou.Lei@colorado.edu

Abstract: The altitude dependence of the upper atmosphere density in response to the variations of solar flux (with 27-day rotation period) and the recurrent geomagnetic activity (with the periods of several days) is investigated on the basis of the accelerometer drag data on board of several satellites during the solar minimum of solar cycle 23. In this study, we used the neutral density data at the reference perigee heights varying from 220 to 450 Km. We found that the density showed significantly different characteristics in response to the solar and geomagnetic forcing at different altitudes. At the same time, the local time and seasonal dependence of the thermospheric density response to the solar and geomagnetic forcing is also discussed.

SOLA-15 Tail and ionospheric signatures of tail fast flows associated with PBIs and with substorms - by Yong Shi, presented by Larry Lyons

Status of First Author: Non-student

Authors: Y. Shi (1), E. Zesta (2), L. Lyons (1), V. Angelopoulos (3), E. Donovan (4), J. P. McFadden (5), C.W. Carlson (5), K.H. Glassmeier (6), and S. Mende (5)

(1) UCLA, Department of Atmospheric and Oceanic Sciences, Los Angeles (yongshi@atmos.ucla.edu)

(2) AFRL/RVBXP, Hanscom AFB, MA

(3) UCLA, Department of Earth and Space Sciences, Los Angeles

(4) University of Calgary, Physics Department

(5) UCB Space Sciences Laboratory, University of California at Berkeley

(6) Technical University of Braunschweig, Braunschweig, D-38106, Germany

Abstract: Earthward convection of the tail plasma sheet is often organized in bursts of fast ion flows restricted in azimuthally narrow channels. It has been shown that Auroral Poleward Boundary Intensifications (PBIs) are often the ionospheric signature of such fast flow channels in the midtail. Equatorward flow bursts have been observed in the ionosphere, and have been shown to be the ionospheric mapping of the tail fast flow channels in few case studies. We focus on identifying such ionospheric signatures and understanding the physics of this magnetosphere-ionosphere interaction via conjunctions of the THEMIS probes with the Sondrestrom radar. We find fundamental differences between the tail fast flows that are associated with substorm onsets and those associated with PBIs, as well as between their respective ionospheric flow signatures. The tail fast flows that produce PBIs are observed in the midtail. They do not typically penetrate to the inner magnetosphere and they are accompanied by plasma sheet expansion signatures in the mid tail. No dipolarization signatures are observed in the inner magnetosphere. The ionospheric signatures associated with such tail flows are PBI-type aurora and substantially enhanced equatorward flows. Tail fast flows that are associated with substorm onsets are typically observed only by the inner magnetosphere probes, only occasionally being seen also in the midtail. Clear dipolarizations are seen with such flows in the inner magnetosphere but not in the midtail. The ionospheric flow associated with such tail fast flows is far distinct, enhanced westward flows being occasionally seen at the higher latitude part of the Sondrestrom field of view with enhanced eastward flows generally observed at the lower latitudes. Enhanced equatorward flows are not seen.

SOLA-16 Effective Aperture Behavior of Open Magnetic Field Lines in the Geospace Environment and on the Sun - by Russell Stoneback

Status of First Author: Non-student

Authors: Russell Stoneback

Abstract: Based upon the similarity of observed fields in the polar ionosphere and an aperture in a conducting plane, a model is presented whereby open magnetic field lines are treated as effective apertures. The use of an effective aperture in the polar ionosphere correctly predicts the frequency dependence of reflected power during the main phase of a geomagnetic substorm as measured by FAST, and is consistent with observed phase speeds. The resonances of the proposed system are consistent with ground based magnetometer measurements and the computed transmission spectra of the Ionospheric Alfvén Resonator (IAR). Applied to the solar polar coronal hole, the use of an effective aperture yields a peak in power transmitted from the chromosphere to corona with a 5 min. period, consistent with observed coronal Alfvén waves using Hinode. The predicted wavespeed of the fast mode for the solar resonator is at 760 km/s, consistent with the fast solar wind speed. Treating a sunspot as an effective aperture predicts umbral 3 min. waves and a temperature range of 4200-5000 K for a photosphere temperature of 5800 K. In the penumbra, the period of these waves approach 8 min.

SOLA-17 Fabry-Perot measurements of H-alpha emissions at Arecibo observatory during geomagnetic storms - by Serge Minin

Status of First Author: Student NOT in poster competition PhD

Authors: Serge Minin, Robert Kerr, Pedrina Santos, John Noto, Michael Migliozi, Juanita Riccobono, Lara Waldrop, Raul Garcia, Farzad Kamalabadi

Abstract: A significant enhancement of H-alpha airglow emission (excited by solar Lyman-beta photons) as a consequence of geomagnetic disturbances has previously been reported by Kerr et al. in a 2001 publication. In the current presentation we revisit the same data sets and analyze them to consider, in addition to the narrow solar excited emission, the enhancements in the broader emission that appear largely as background enhancements in the measured spectra. The broad emission enhancement could be indicative of enhanced collisional excitation rates (such as low latitude auroral excitation). We also present data collected during two more recent storms using an updated instrument configuration with sensitivity enhanced by use of CCD detection.

Instruments or Techniques for Ionospheric or Thermospheric Observation

ITIT-01 Uncertainties in extracted Gaussian emission line parameters: measurement setup choices in Doppler spectroscopy with continuum background - by Serge Minin

Status of First Author: Student IN poster competition PhD

Authors: Serge Minin, Farzad Kamalabadi

Abstract: We have derived analytical expressions for uncertainties in parameters extracted by nonlinear least squares fitting of a Gaussian emission function with a significant continuum background component. The formulas have been verified with numerical simulations. The analytical expressions can be used to estimate lower bounds of error in Fabry-Perot Doppler spectroscopy. Effects of certain choices in measurement setup and analysis are investigated.

ITIT-02 Multi-purpose Radar Controller - by Alexander Hackett

Status of First Author: Student IN poster competition Undergraduate

Authors: Alexander Hackett - Penn State University, Ryan Seal - Penn State University, Dr. Julio Urbina - Penn State University, Sixto Gonzalez - Arecibo Observatory, Mike Sulzer - Arecibo Observatory

Abstract: The Multi-purpose Radar Controller is an FPGA based system, using a variety of open source tools. The project contains two distinct programs: the bit pattern generator and the shell program. The former is not specifically designed for the Arecibo Observatory radar controller; rather, it is designed to be a "general-purpose" bit pattern generator that may generate test patterns for any digital project. To accomplish such a task, a language parser for C++, found in the Boost library, was used to translate system specific information into bit vectors, used to initialize the FPGA before operation. The shell program acts as a user interface during operation of the controller. It is a multithreaded piece of software, allowing the user to change bit patterns sent to the FPGA, start and stop the system, and access several other options relating to the FPGA's operation. Utilizing another portion of the Boost library, networking capability allows remote operation of the system.

ITIT-03 Statistical analysis of high-latitude F-region ionospheric composition - by Benjamin Adams Burnett

Status of First Author: Student NOT in poster competition Undergraduate

Authors: Benjamin Burnett - Boston University - bburnett@bu.edu, Matt Zettergren - Boston University - mattz@bu.edu, Joshua Semeter - Boston University - jls@bu.edu

Abstract: Strong perpendicular electric fields are a common feature of high latitude ionosphere. High ionospheric temperatures at low altitudes often correspond with these electric fields and can drastically change the chemical composition of the ionosphere. Under these conditions, ion temperature data derived from ISR measurements disagrees with theoretical model calculations. This indicates a discrepancy in the ISR data-fitting model which is most likely explained by an incorrect model of ion masses. A statistical survey of Sondstrom data between 1998 and 2001 demonstrates systematic disagreement between measured and modeled ion temperature profiles. These data are also used to investigate the measured relationship that electric field has with these ion heating events, through a comparison of direct E-field measurements from 3-position mode experiments with indirect, calculated measurements based on conservation of energy. A new method to estimate ion composition from ISR data is then applied to a large database of measurements from high-latitude ISR measurements. This analysis is used to study factors contributing to ion composition variability, including electric fields, neutral atmospheric changes, and precipitating particles.

ITIT-04 Validation of IDA4D estimates of F-region electron densities using CHAMP in-situ and ground-based ionosonde observations of electron density - by Gary S Bust

Status of First Author: Non-student

Authors: G. S. Bust, ASTRA, San Antonio, TX, R. L. Bishop, Aerospace, El Segundo, CA, P. R. Straus, Aerospace, El Segundo, CA, G. Crowley, ASTRA, San Antonio, TX, A. Reynolds, ASTRA, San Antonio, TX, N. Curtis, ASTRA, San Antonio, TX

Abstract: An approach is presented to validate the accuracy of Ionospheric Data Assimilation Four Dimensional (IDA4D) estimates of electron density using independent measurements of electron density in the F-region of the ionosphere. The primary data source used as independent "truth" was in-situ measurements of electron density from the CHAMP satellite (~ 400 km altitude orbit). As a secondary data source, ionosonde observations of NmF2 were also used.

The approach used a month long set of data and IDA4D results. The IDA4D results were interpolated onto the CHAMP positions and times for each measurement throughout the day (~ 6000 observations per day). Statistics were computed for the average, standard deviation and rms errors in IDA4D as compared with the "truth" observations. Both absolute and relative (percent) errors were computed. In addition to estimating electron density, IDA4D produces a formal estimate of the expected 1-sigma standard deviation of error in the electron density estimates. This IDA4D estimate of error was also validated using the same data sets, to determine whether the formal error-bars produced by IDA4D are reliable tracers of the 1-sigma error levels of electron density in the F-region of the ionosphere.

The results of this study represent the first systematic attempt to characterize the accuracy of IDA4D electron density products at specified altitudes in the F-region of the ionosphere. IDA4D is used in a number of ongoing scientific studies. The results of this validation effort can be used as a guide to inform researchers of the expected accuracies of IDA4D in these scientific studies.

ITIT-05 Numerical Predictions on Mid-Latitude Ionospheric Locations - by Eli Hibit

Status of First Author: Student IN poster competition PhD

Authors: Eli Hibit, Dr. Julio Urbina, Dr. Lars Dyrud

Abstract: A linux-based numerical code is using non-specular meteor data drawn from 2 mid-latitude sites to make predictions about incoming masses and velocities based on trail duration and average height.

ITIT-06 The NorthEast CIDR Array: A new chain of ionospheric tomography receivers for studying the equatorward edge of the auroral oval and the mid-latitude trough - by Hugh A Gallagher, presented by Allen Weatherwax

Status of First Author: Non-student

Authors: Hugh Gallagher, Peter Anderson, Luke D'Imperio, Timothy Kelly, SUNY Oneonta, Trevor Garner Applied Research Laboratory, University of Texas, Austin, Allan Weatherwax, James Akey, Siena College

Abstract: An array of five Coherent Ionospheric Doppler Receivers (CIDRs) has been established in the North Eastern United States. Four of the receivers are distributed over approximately 400 km of longitude at about 54° geomagnetic latitude. A fifth receiver has been deployed south of the primary chain at Wallops Island. This summer a sixth receiver will be positioned north of the primary array in the Adirondack Mountains. The North East CIDR Array makes observations of total electron content (TEC) and the rate of TEC (ROT) fluctuations obtained from VHF and UHF beacons on low-earth-orbiting satellites. In this poster, we will present initial observations of TEC and ROT made by the CIDRs. Additionally, we will examine variations in TEC and ROT over the longitudinal extent of the array.

ITIT-07 An Auroral Scintillation Observation using Precise Collocated GPS Receivers
by Trevor W Garner

Status of First Author: Non-student

Authors: T W Garner (garner@arlut.utexas.edu) and R B Harris, Applied Research Laboratories, Univ. of Texas, C S Herbst and C F Minter, National Geospatial-Intelligence Agency

Abstract: A short scintillation event occurred on January 10, 2009 between 9:23 and 9:26 UT. A three-receiver GPS ground station at Fairbanks, Alaska experienced a loss of lock with PRN 3 on 2 of three collocated GPS receivers. The third receiver tracked through the scintillation event. Even though it was geomagnetic quiet, a significant plasma enhancement is observed with a 7 TECu enhancement over less than 20 km

ITIT-08 The First Result of Coherent Ionospheric Doppler Receiver Measurements over Egypt - by
Ayman Mahrous, presented by Trevor Garner

Status of First Author: Non-student

Authors: A. M. Mahrous and A.A.Shimeis, Helwan University and T. W. Garner, Applied Research Laboratories, University of Texas

Abstract: This paper presents the first results obtained Total Electron Content (TEC) measurements over Egypt taken by UHF/VHF receivers. Such ionospheric measurements over the Middle East and North Africa have been previously unable to the scientific community, but are now available for ionospheric studies. In particular, these receivers are well situated to study the northern peak of the equatorial anomaly. This initial study examines the behavior of the anomaly during two magnetic storm periods (12 July and 11 October 2008). The response of the northern equatorial anomaly crest is examined through these minor storms, one at solstice and the other at equinox, using ionospheric total electron content (TEC) measurements from a Coherent Ionospheric Doppler Receiver (CIDR) at Helwan, Egypt (29.8641 N, 31.3172 E). Particular attention is shown to diurnal changes in the crest structure and to the response to the changing magnetic conditions.

ITIT-09 Observations of the auroral electrojet plasma using UHF/VHF radio beacon measurements -
by Stephen Bayne

Status of First Author: Student NOT in poster competition Undergraduate

Authors: S Bayne and H Gallagher, State University of New York -Oneonta, T W Garner, Applied Research Laboratories, University of Texas, A T Weatherwax, Siena College, J Secan, Northwest Research Associates

Abstract: This poster presents observations of a plasma structure that corresponds to auroral electrojet current. TEC observations from a chain of UHF/VHF receivers in Alaska indicate the presence of an E-region plasma enhancement. This enhancement correlates to the location of the auroral electrojet determined from a coincident ground magnetometer chain.

ITIT-10 Development, Simulations, and Validations of CubeSat Retarding Potential Analyzer - by Ryan Davidson

Status of First Author: Student NOT in poster competition Masters

Authors: Ryan L. Davidson, G. D. Earle, J. Klenzing

Abstract: CubeSats are quickly moving away from being the subjects of viability tests and towards being useful atmospheric science tools. A plan for development of a retarding potential analyzer capable of flight aboard a CubeSat is presented. A mechanical design has been produced and a prototype is under construction. Simulation and experimental validation of varying grid geometries is underway.

ITIT-11 Remote Oxygen Sensing by Ionospheric Excitation (ROSIE) - by Konstantinos S. Kalogerakis

Status of First Author: Non-student

Authors: K. S. Kalogerakis (SRI), T. G. Slanger (SRI), E. A. Kendall (SRI), T. R. Pedersen (AFRL), M. J. Kosch (Lancaster U.), B. Gustavsson (U. Tromso), M. T. Rietveld (EISCAT)

Abstract: The principal optical observable emission resulting from ionospheric modification (IM) experiments is the atomic oxygen red line at 630 nm, originating from the O(1D - 3P) transition. Because the O(1D) atom has a long radiative lifetime, it is sensitive to collisional relaxation and an observed decay faster than the radiative rate can be attributed to collisions with atmospheric species. In contrast to the common practice of ignoring O-atoms in interpreting such observations in the past, recent experimental studies on the relaxation of O(1D) by O(3P) have revealed the dominant role of oxygen atoms in controlling the lifetime of O(1D) at altitudes relevant to IM experiments. Using the most up-to-date rate coefficients for collisional relaxation of O(1D) by O, N₂, and O₂, it is now possible to analyze the red line decays observed in IM experiments and thus probe the local ionospheric composition. In this manner, we can demonstrate an approach to remotely detect O-atoms at the altitudes relevant to IM experiments, which we call remote oxygen sensing by ionospheric excitation (ROSIE). The results can be compared with atmospheric models and used to study the temporal, seasonal, altitude and spatial variation of ionospheric O-atom density in the vicinity of heating facilities. We discuss the relevance to atmospheric observations and ionospheric heating experiments and report an analysis of representative IM data.

ITIT-12 Initial Electron Temperature Results from the Planar Langmuir Probe on C/NOFS - by Patrick A. Roddy

Status of First Author: Non-student

Authors: Roddy, Patrick A.; Machuzak, John; Hysell, David; Hairston, Marc; Coley, William R.

Abstract: The Planar Langmuir Probe (PLP) on C/NOFS measures in-situ ion and electron densities as well as electron Temperature and spacecraft potential. PLP has been making Te measurements continuously since May 2008. We present here initial results of the Te measurements from the PLP swept bias probe made during this period of unprecedented solar inactivity. Comparisons the PLP Te with ion temperatures derived from UTD's retarding potential analyzer (also aboard C/NOFS) and electron temperatures obtained from the Jicamarca incoherent scatter radar are also presented.

ITIT-13 Robust GPS Signal Tracking Under Ionosphere Scintillation - by Lei Zhang

Status of First Author: Student IN poster competition PhD

Authors: L. Zhang, X. Mao, Y. Morton, Q. Zhou, Miami University

Abstract: The ionosphere is a highly dynamic medium characterized by irregularities in electron density and hence the medium refractive index. The irregularities of the ionosphere refractive index cause scattering and diffraction of radio waves such as GPS signals that traverse the ionosphere. The results of these signal interaction with the ionosphere are signal amplitude fading and phase fluctuations, collectively called the ionosphere scintillation effects. Numerous studies

have been conducted on ionosphere scintillation theories, climatology, morphology, statistical behavior of both amplitude and phase scintillation signals in a wide range of frequencies, as well as scintillation effects on communication and navigation systems. In the past two decades, GPS receivers have been widely used in monitoring and studying of ionosphere scintillations. Commercially available GPS receivers, however, are not designed to yield optimal performance under scintillation conditions. This poster paper compares several tracking methods performances under ionosphere scintillation using both simulated GPS scintillation signals and real RF samples generated by a GPS receiver under scintillation conditions. These methods include the conventional carrier phase lock loop, a Kalman filter-based phase estimator, and a batch-based open loop tracking method. Different levels of scintillations and GPS signal carrier to noise ratios will be evaluated using these methods.

ITIT-14 The LISN database: Description and initial results - by Cesar De La Jara

Status of First Author: Student NOT in poster competition Undergraduate

Authors: C. De La Jara, J. L. Chau, J. C. Espinoza, O. Veliz, C. Valladares, T. Bullet, R. Livingston

Abstract: A set of complementary instruments (GPS, magnetometers and ionosphere sounders) has been deployed in the South American region to study the electrodynamics of the low-latitude ionosphere and upper atmosphere, as part of the LISN project. The automatic data collection that this network of sensors performs, is complemented with the implementation of a database for storing, processing and retrieving collected information. In this work, we describe the characteristics of our database, including information about quality control, data access, on-line plotting routines, etc. Special emphasis is given to the presentation of VIPIR (ionosonde) results, obtained with a variety of modes. Among other modes, we show preliminary results of special modes to study the equatorial E and valley region and the highly dynamic F region around sunrise and sunset times.

ITIT-15 First Observations of Equatorial TEC and Scintillation with Multiple Dual-Frequency Software-Defined GPS Receivers - by Brady O'Hanlon

Status of First Author: Student IN poster competition PhD

Authors: Brady O'Hanlon, bwo1@cornell.edu, Cornell University, Paul Kintner, pmk1@cornell.edu, Cornell University. Eurico R, de Paula, eurico@dae.inpe.br, Instituto Nacional de Pesquisas Espaciais

Abstract: A dual-frequency software-defined GPS receiver has been developed and used for monitoring total electron content (TEC) and observing equatorial ionospheric scintillation. The Cornell University GPS Receiver Implemented on a DSP (GRID) utilizes the GPS L1 C/A and L2 C signals to measure TEC and observe scintillation. The GRID receiver measured TEC and GPS signal amplitude and phase at 10 Hz. Also employed were two similar GPS digital storage receivers (non-real-time) that made the same measurements at 50 Hz. These receivers were arranged in a linear array and utilized in January, 2009 in Natal, Brazil (magnetic latitude 2.42°) to make these observations. Mild scintillation of the L1 C/A and L2 C signals was observed. TEC measurements agreed well with those taken by a collocated GPSV 4004B Scintillation/TEC Monitor. We demonstrate the use of multiple receivers to measure drifts, report on the first fast (10Hz-50Hz) multiple receiver TEC measurements in the equatorial ionosphere, and discuss the capabilities of the GRID.

ITIT-16 Application of Bayesian Spectral Analysis to SuperDARN ACF Data - by Jeffrey Spaleta

Status of First Author: Non-student

Authors: J. Spaleta, UAF/GI; R. T. Parris, UAF/GI; W. Bristow, UAF/GI

Abstract: The SuperDARN radars make use of a multi-pulse sequence technique to achieve high velocity resolution over a significant range extent. The problem of cross range interference inherent in the multi-pulse technique is mitigated by analysis of averaged auto correlation functions (ACFs). The individual ACFs are constructed from the backscatter returns, taking pairs of pulses in a single multi-pulse sequence. When multiple ACFs are averaged, the uncorrelated cross range inference is rejected.

These average ACFs are then fitted using a special purpose FitACF algorithm. The FitACF algorithm calculates Doppler velocities and spectral widths assuming a single velocity target and can not easily account for multiple velocity targets from

the same range volume. Such situations are thought to commonly occur at ranges where ground scatter and ionospheric scatter are mixed. A Bayesian parameter estimation technique is being investigated for suitability for recovering ACF spectral information not obtainable with the FitACF algorithm. This technique is suitable for extracting spectral information concerning a wide range of model functions including the non-stationary model functions currently used in the FitACF algorithm. This poster focuses on the application of the Bayesian technique on existing SuperDARN ACF data, with an emphasis on a comparison to the results of the existing FitACF analysis.

ITIT-17 Imaging with the Kodiak Island SuperDARN HF Radar - by Richard Todd Parris

Status of First Author: Student IN poster competition PhD

Authors: W. A. Bristow, Geophysical Institute, University of Alaska Fairbanks

Abstract: The Kodiak Island radar was upgraded with an imaging receiver system and a direct digital synthesis beam-forming system in 2008. This upgrade replaced the phasing matrix and now treats each antenna as an independent sensor. Recording the echo signal at each antenna permits the application of imaging techniques and can yield more detailed information about the distribution of radar targets in the field-of-view of the radar. This poster will discuss the imaging techniques that have been applied on the Kodiak radar and will provide some recent observations along with a discussion about the benefits of radar imaging for SuperDARN.

ITIT-18 Simultaneous radar measurements of daytime zonal and vertical plasma drifts in Peru and Brazil - by Fabiano S Rodrigues

Status of First Author: Non-student

Authors: F. S. Rodrigues, ASTRA, San Antonio – TX; E. R. de Paula, INPE, Sao Jose dos Campos, SP, Brazil; D. L. Hysell, Cornell University, Ithaca – NY; J. L. Chau, Jicamarca Radio Observatory, Lima, Peru

Abstract: It has been shown that the vertical Doppler velocity of the so-called 150-km echoes is a good proxy of the equatorial F-region vertical plasma drifts and suggested that small radar observations of the 150-km echoes could be used to monitor these drifts [e.g. Kudeki and Fawcett, 1993]. These 150-km echoes have been detected by a small, low-power 30 MHz coherent scatter radar in Sao Luis, Brazil (2.59 deg. S, 44.21 deg. W, -2.35 dip lat).

An approach to estimate the vertical and zonal components of the Doppler velocity of these echoes using two spaced antennas is described and applied to observations made by the Sao Luis radar.

Examples of the results showing the daytime variation of zonal and vertical drifts over Sao Luis are presented and compared with 150-km echoes drifts measured at Jicamarca on the same day.

To our knowledge, these are the first radar measurements of daytime vertical and zonal drifts in the Brazilian sector.

ITIT-19 An alternative approach for estimating E-region density profiles from GPS radio occultation measurements - by Fabiano S Rodrigues

Status of First Author: Non-student

Authors: F. S. Rodrigues, ASTRA, San Antonio, TX; M. J. Nicolls, SRI International, Menlo Park, CA; G. S. Bust, ASTRA, San Antonio, TX; J. L. Chau, Jicamarca Radio Observatory, Lima, Peru

Abstract: An approach for estimating E-region density profiles is presented. It combines the F-region electron density results of an assimilative model of the ionosphere and measurements of GPS radio occultation. The model results are used to estimate and subtract the F-region contribution to the total electron content (TEC) measured by the occultations. The resulting E-region TEC is then inverted using the inverse Abel transform.

The methodology is applied to COSMIC occultation measurements, and uses F-region density estimates from the Ionospheric Data Assimilation Four-Dimensional (IDA4D) algorithm. The inversion results are compared with IRI and FIRI model predictions of E-region density profiles, and with E-region density profiles measurements made by the Jicamarca-Paracas bistatic radar system near the magnetic equator in Peru.

A good agreement between the hmE and fofE parameters of the inverted profiles, model (IRI and FIRI) predictions, and radar measurements was found. We were able to identify the daytime (0800 – 1700 LT) variation of the E-region densities using the inversion results suggesting the robustness and relatively low uncertainties of the inversions.

ITIT-20 Amplitude modulation for Arecibo F-region ISR experiments - by Romina Nikoukar

Status of First Author: Student NOT in poster competition PhD

Authors: Romina Nikoukar, Farzad Kamalabadi, Michael Sulzer, Erhan Kudeki, and Sixto Gonzalez

Abstract: The current standard technique for estimation of F-region ionospheric parameters at Arecibo involves simultaneous long pulse transmissions over multiple frequencies [Sulzer, 1986]. This technique has been developed to take advantage of the high Signal-to-noise ratio achievable in the F-region Arecibo measurements. The range smearing of information caused by the long pulse modulation, however, is inevitable and as such the range resolution is very coarse (about 38 km).

In this work, we study the performance of amplitude modulation in Arecibo incoherent scatter radar (ISR) experiments in terms of statistical accuracy and range resolution. We choose amplitude modulation for this study because amplitude modulation results in lower correlation between autocorrelation function lag estimate errors, which in turn introduces a higher level of accuracy in estimated ionospheric parameters when measurements are integrated in range. To investigate the performance of amplitude modulation in terms of range resolution and to envision the inherent trade-off between estimation accuracy and resolution we exploit mathematical measures currently used as model order selection methods. We examine these techniques on Arecibo ISR measurements utilizing amplitude modulation, and we find that compared with an unmodulated long pulse, either similar range resolution with increases statistical accuracy or similar accuracy with finer range resolution can be obtained.

ITIT-21 Understanding Biases in Atmospheric Density Derived from Satellite Drag by Marcin Pilinski

Status of First Author: Student IN poster competition Masters

Authors: Marcin Pilinski, University of Colorado at Boulder, marcin.pilinski@colorado.edu

Abstract: Much of our knowledge of the neutral thermospheric structure stems from investigations of aerodynamic forces on satellites in low earth orbit. Such measurements are a convolution of the satellite drag coefficient, cross sectional area, and mass, referred to as the ballistic coefficient, with the free stream velocity, atmospheric temperature and mean molecular mass. An important variation in the first parameter results from a change in the nature of gas-surface interactions which is believed to be driven by atomic oxygen adsorption to the satellite surface. Here, we examine the dependence of the drag coefficient on various parameters including those which commonly vary due to the effects of space weather and comment on the consequences for the deduction of atmospheric densities. One particularly salient feature which results from recent understanding of satellite gas-surface interactions is that enhancements in density may be associated with a drop in the drag coefficient, leading to an underestimation of the actual density during geomagnetic events. The dependence of measured density uncertainty is also explored as a function of satellite shape and cross sectional area. Drag coefficient variability is related to the thermospheric wind structure and this in turn varies with latitude. We will therefore examine how drag measurements may vary with latitude. Also, the extent to which averaging density over an orbit results in unwanted biases resulting from orbital alignment is explored. Finally, a satellite mission being readied for flight at the University of Colorado is presented which will address some of these uncertainties and pave the way for improved neutral density measurements.

ITIT-22 Advanced techniques of tomographic reconstruction algorithms for observing the night time ionospheric air glow – Steven Burr

Status of First Author: Student NOT in poster competition

Authors: Steven Burr, burrguy@gmail.com, Todd K. Moon, todd.moon@engineering.usu.edu, Charles M. Swenson, charles.swenson@usu.edu

Abstract: Utah State University has been exploring the mission and instrument requirements for tomographic observations of ionospheric air glow. Such a mission would employ a rotating field of view photometer making line of sight measurements and using tomographic processes to produce a two dimensional cross section of the atmosphere. The tomographic reconstruction method is based upon the natural pixel representation and a relatively fast implementation has been developed in both MatLab and C. In this formulation, image reconstruction requires solution of a large nonsparse set of equations involving a Grammian matrix whose elements depend upon the geometry of the orbit and region being imaged. We present detailed discussion of how to stably compute the elements of the Grammian matrix and an efficient algorithm for reconstructing the image from the projection weights. Advanced techniques are also presented on using in situ measurements and assumptions based on atmospheric features to improve the accuracy of the images. Results on simulated data indicating spatial resolution and contrast will be presented for various sensor parameters. Emphasis is placed on the possibility of observing equatorial plasma bubble signatures from a small satellite using 135.6 nm emissions from Oxygen ion recombination.

ITIT-23 RAIDS: A New Mission for Ionospheric and Lower Thermospheric Science
by Andrew Stephan

Status of First Author: Non-student

Authors: Andrew Stephan (NRL), Scott Budzien (NRL), Rebecca Bishop (Aerospace), Paul Straus (Aerospace), Andrew Christensen (Aerospace), James Hecht (Aerospace)

Abstract: The Remote Atmospheric and Ionospheric Detection System (RAIDS) is a suite of three photometers, three spectrometers, and two spectrographs measuring key thermospheric and ionospheric airglow features across the wavelength range 50-874 nm. RAIDS is manifested for launch to the Japanese Experiment Module-Exposed Facility aboard the International Space Station (ISS) in 2009. The primary scientific objectives of the RAIDS experiment are to study the temperature of the lower thermosphere (100-200 km), and to measure composition and chemistry of the lower thermosphere and ionosphere. We highlight these new measurements that RAIDS will obtain and their potential contribution to our understanding of the ionosphere-thermosphere system in concert with current and future space- and ground-based experiments.

ITIT-24 Design of a Digital Pulsed Radar Receiver: Increasing Aeronomy Observation Bandwidth at Arecibo Observatory - by Matthew D Sunderland

Status of First Author: Student IN poster competition Undergraduate

Authors: Matthew Sunderland: Penn State University, Julio Urbina: Penn State University, Michael Sulzer: Arecibo Observatory, Sixto Gonzalez: Arecibo Observatory

Abstract: Digital electronics have revolutionized communications and signal processing applications. The increased speed and capability of modern FPGAs and ADCs have enabled larger bandwidth signals to be processed in the digital domain. When applied to radar aeronomy applications, this has resulted in increased bandwidth combined with greater flexibility. We present a design of an FPGA-based pulsed radar receiver for ionospheric research that significantly increases bandwidth over existing systems. Based on hardware developed for pulsar detection, the reconfigurable FPGA-based platform is reprogrammed to perform pulsed radar aeronomy observations by IF sampling of the Arecibo 430-MHz radar.

ITIT-25 Optimization of GC314 Digital Receiver - by Sandeep Anna Kor

Status of First Author: Student NOT in poster competition Masters

Authors: Sandeep Kor, Dr. Julio Urbina

Abstract: In recent years, the rapid emergence of new standards and protocols in wireless communication has led to the rapid development of digital receiver technology. Advances in this technology make now possible the implementation of modern acquisition systems based in digital receivers. In this poster we describe the implementation of a Linux-based device driver for the Echotek ECDR-GC314-PCI-FS commercial off the shelf 12 channel digital receiver system. We will describe the architecture of the digital receiver and the software principles used to design and implement the system. We will also present preliminary results of the deployment of this system in conjunction with the new meteor radar being developed at Penn State.

ITIT-26 Estimation of Langmuir Probe Currents in the event of Surface Potential Variation - by Padmashri Suresh

Status of First Author: Student IN poster competition Masters

Authors: Padmashri Suresh,Utah State University, Dr. Charles M Swenson,Utah State University

Abstract: Langmuir probes are diagnostic instruments widely used in the measurement of plasma parameters in the Ionosphere. Theories for the current collected by a probe are the most essential factor in the accurate computation of plasma parameters. The current is a function of the probe potential measured with respect to the surrounding plasma. Unexpected, or theoretically unaccounted for variations in this potential affect current measurements, which in-turn influence the computation of plasma parameters. Spatial variations of work function across the probe surface have been observed due to non-uniformity of crystalline surface properties and by factors such as ‘surface contamination’ of the probe.

The theoretical expressions for the ‘collected current’, currently available in literature, do not consider these factors as first principles. Hence in the event of surface potential variations, the plasma parameters computed using the currently available mathematical models will be erroneous.

We present a mathematical model of currents collected by Langmuir probes as a function of surface potential variations. An analysis and mathematical formulation of the probe current for flat plate, cylindrical and spherical probes are presented for the case of varying surface potential. We also present the results of the analysis of our model for a probe flown on a sounding rocket and a probe located on the international space station.

ITIT-27 The role of geomagnetic field on the occurrence of specular meteor trails - by Siming Zhao

Status of First Author: Student NOT in poster competition Masters

Authors: Siming Zhao, Dr. Julio Urbina, Dr. Lars Dyrud

Abstract: In this poster, we studied the observations from a 50MHz radar stationed near Salinas, Puerto Rico. The radar system has two sub-arrays with one beam perpendicular to the earth magnetic field and the other one off perpendicular to the earth magnetic field both at an elevation angle of approximate 41 degrees. In our data, two types of echoes from meteor trails can be observed: specular reflections from trails oriented perpendicular to the radar beam and non-specular reflections from trails deposited with arbitrary orientations. We compared the reflected echoes from the two radar receivers and studied how the magnetic field may affect the observation of specular trails as well as the non-specular trails.

ITIT-28 Ionospheric measurements from LWA calibration - by Christopher Watts

Status of First Author: Non-student

Authors: Christopher Watts, University of New Mexico, cwatts@ece.unm.edu; Aaron Cohen, Naval Research Lab, Aaron.Cohen@nrl.navy.mil; Patrick Crane, Naval Research Lab, pcrane@ccs.nrl.navy.mil, representing the Long Wavelength Array

Abstract: The Long Wavelength Array (LWA) is a new telescope/interferometer facility being established to do astrophysical observations in the frequency range 10 MHz to 90 MHz. As such, measurements will be strongly affected by the ionosphere. “Calibration” of the LWA is designed to remove distortions caused by the ionosphere; however, this data can be used as a new tool for high resolution measurements of the ionosphere. In fact, part of the LWA mandate is to make highly precise measurements of the ionosphere. The current calibration scenario calls for the rapid monitoring (every 10 s) of ~100 known “calibrator” stars. We are currently testing this technique through modeling, in order to place limits on the complexity of ionospheric structure that can be compensated for. Results will be presented.

ITIT-29 Estimation of Temperature and Wind Velocity Profiles in Upper Atmosphere Using Fabry-Perot Interferometers - by Yiyi Huang

Status of First Author: Student IN poster competition PhD

Authors: YiYi Huang

Abstract: The temperature and neutral wind velocity are two important state parameters of the upper atmosphere. The Fabry-Perot Interferometer (FPI) is an instrument that facilitates for the estimation of these parameters from the observations of the Doppler shift and broadening of naturally-occurring airglow emissions. In this poster, we present a forward model that simulates what FPI observations, allowing us to test analysis and inversion algorithms under a variety of conditions. We develop this forward model for the emission at 630.0 nm that arises from the dissociative recombination O_2^+ in the thermosphere/ionosphere. The forward model is based on existing climatological models of the thermosphere and ionosphere and a physical model of the FPI. We present a simulation of a ground-based FPI which matches quite well with actual FPI data collected from a FPI operated at the Urbana Atmospheric Observatory. We then generalize the model and simulate different observing configurations, including a satellite-based FPI. Finally, we use the model to investigate the feasibility of obtaining altitude profiles of the neutral wind and temperature using a cluster of FPIs observing a common atmospheric volume.

ITIT-30 Higher Order Ionosphere Error in GPS Measurements - by Priyanka Chandrasekran, presented by Yu Morton

Status of First Author: Student NOT in poster competition Undergraduate

Authors: Priyanka Chandrasekran

Abstract: The high variability of the Earth’s ionosphere is an important source of range error for Global Positioning System (GPS) measurements. Current dual-frequency GPS receivers eliminate the first order ionosphere error. Understanding of the higher order errors is critical for many precision applications like weapon guidance, navigation and tracking, surveying, agriculture, and search and rescue operations. The objective of this study is to assess the temporal and spatial structure of second order error in GPS range measurements using joint GPS and Incoherent Radar measurements.

Data Assimilation

DATA-01 Ionosphere geomagnetic field: comparison of IGRF model prediction and satellite measurements - by Nick Matteo, presented by Yu Morton

Status of First Author: Student NOT in poster competition Masters

Authors: Nick Matteo, Yu Morton, Electrical and Computer Engineering, Miami University, mortonyt@muohio.edu

Abstract: The geomagnetic field is an important parameter in the ionosphere. The IGRF model is designed to model the Earth main field and the Gauss coefficients of the IGRF model are based on ground-based magnetometer measurements. Various current sources in the ionosphere may alter the actual B field distribution in the ionosphere. Direct measurements of the ionosphere geomagnetic field are needed to validate the performance of the IGRF model in the ionosphere.

Several satellite missions were launched during the past decade specifically aimed to study ionosphere geomagnetic field in the altitude range of 100 to 1000 km. We have analyzed some of the magnetometer data collected on board these satellites and compared the data with that of the IGRF predictions. Our preliminary results indicated that the IGRF model is within 1% accuracy of the measured ionosphere B field. Detailed analysis of studies under varying solar conditions will be presented based on data taken from the following satellites: Argentine Commission on Space Activities (SAC-C), DEMETER, Orsted, and CHAMP.

DATA-02 An Expert System for Ionogram Reduction (ESIR) - by Donald D Rice

Status of First Author: Non-student

Authors: D. D. Rice, J. J. Sojka, and D. C. Thompson, Space Environment Corporation , sec@spacenv.com

Abstract: The Expert System for Ionogram Reduction (ESIR) uses knowledge-guided pattern recognition algorithms designed for finding the primary ionospheric layers E, F1, and F2 in standard virtual height versus frequency ionograms. The system can analyze mid- and low-latitude ionograms, and is able to assess the presence of sporadic E and spread F. ESIR can accept ionograms from various sources, including scans of archival film and prints, as well as modern digital files. ESIR is designed to produce ionogram inversions leading to electron density profiles (EDP) for users who need very high reliability in the product quality control.

ESIR has been developed to mimic the expertise of the ionogram hand scaler. The expert hand scaler is guided by knowledge of the ionosphere and the recognition of reasonable patterns when unscrambling the desired ionospheric signature from a proliferation of other information and interference in an ionogram. Useful information is obtained by considering the overall distribution of points forming reasonable traces. The challenge for automated algorithms is to see those patterns and thus discern “the tree in the forest.” Furthermore, the expert hand scaler determines whether the ionogram has a clean, reliable signature or if it is noisy and unreliable, and provides the user with this information. Similarly, the design objective of the ESIR team is that ESIR results always include quality information that is both qualitative and quantitative. This is achieved by comparing multiple solutions to obtain a more complete view of the solution phase space, enabling quality assessments to be made. If ESIR is unable to reliably analyze an ionogram, it will report a null result, rather than generating suspect scaling data.

Space Environment Corporation currently has a patent pending on the ESIR technology.

DATA-03 The Madrigal database at Jicamarca Radio Observatory: Data from the main instruments of Jicamarca available to the world - by Juan Urco Cordero

Status of First Author: Student NOT in poster competition Undergraduate

Authors: M. Urco, B. Rideout, P. Bravo

Abstract: Jicamarca currently has several databases, each with data from a specific experiment. Madrigal has been selected as the unique manager and server archival, it as part of the process of unification and standardization of existing databases in the JRO. Madrigal is an upper atmospheric science database most used around of the world and in this work we describe the characteristics of our database, including its installation and configuration. Special emphasis is given to the development of the custom interface to access Jicamarca data.

DATA-04 Dagik: Data-showcase system for the geospace using Google Earth - by Akinori Saito, presented by Michi Nishioka

Status of First Author: Non-student

Authors: Akinori Saito, Michi Nishioka and Daiki Yoshida; Kyoto University

Abstract: The recent development of geo-browsers, such as Google Earth and NASA World Wind, makes it possible to plot various types of data in four dimension, that is three-dimension in space and one-dimension in time. The data presentation on these geo-browsers is a powerful tool to compare and combine the ground-based and space-borne observational and model-generated data. Dagik is a system to share the geospace data plot on Google Earth. Many types of data, such as GPS-TEC, EISCAT, Super-DARN, IMAGE-FUV, DMSP ion density, ground-based magnetometer, solar wind, and indices are now available on Dagik. This is a system to display data of databases on the geo-browser. The users who are interested in the data follow the network link and access to the database. Therefore we call this system is a data-showcase system. We introduce the concepts of Dagik and demonstrate some examples of plots on Dagik in the presentation.

Equatorial Ionosphere or Thermosphere

EQIT-01 Preliminary Comparison of In-Situ Plasma Density Structures from C/NOFS at Dusk with TEC and Scintillation Data from LISN obtained during October 2008 by Michi Nishioka

Status of First Author: Student NOT in poster competition PhD

Authors: M.Nishioka, Su. Basu, C. Valladares and S. Basu; Boston College; P. Roddy and K. Groves; Air Force Research Laboratory

Abstract: Preliminary results of simultaneous observations of electron density depletions associated with structured plasma bubbles and total electron content (TEC) variations and scintillations will be presented. The electron density at 400-600 km altitude range in the equatorial ionosphere was measured with a Planar Langmuir Probe (PLP) on the Communications/Navigation Outage Forecast System (C/NOFS) satellite. The C/NOFS satellite flew over the South American sector around the dip equator at dusk in early October, 2008. TEC and L-band scintillation measurements were conducted by the use of Low-latitude Ionospheric Sensor Network (LISN) in South America and this was augmented by VHF scintillation from AFRL's SCINDA (Scintillation Network Decision Aid). The in-situ data revealed the presence of structured plasma density depletions almost everyday at dusk. However the magnitude of scintillation at 250 MHz was critically dependent on the prevailing background density in which the bubbles were observed. Further, the magnitude of TEC fluctuations varied considerably from the magnetic equator to the equatorial anomaly crest but nowhere were they large enough to create significant L-band scintillation. The results of this preliminary study seems to indicate that while bubbles and plumes were prominent on a few days during the October 2008 period, strong scintillation events which impact communication/navigation systems will have to await the return of high plasma densities and large scale heights in the F-region of the equatorial ionosphere.

EQIT-02 Atomic and molecular ion dynamics during equatorial spread F - by Glenn Joyce

Status of First Author: Non-student

Authors: G. Joyce, J.D. Huba*, and J. Krall*, Icarus Research, Inc., Bethesda, MD

*Plasma Physics Division, Naval Research Laboratory, Washington, DC

Abstract: The first simulation study of atomic and molecular ion dynamics during equatorial spread F (ESF) is presented. The simulation results are based on the Naval Research Laboratory SAMI3/ESF three-dimensional code. The key findings are the following: (1) a "super fountain" effect can occur in the initial stage of ESF with upward ion velocities of order 1 km/s, (2) plasma depletions can be enhanced by the "drainage" of H⁺ ions along the geomagnetic field, and (3) molecular ions (e.g., NO⁺) can be "lifted" above the altitudes of the background F layer. Associated with these dynamics are ion temperature enhancements in the "legs" of the ESF "bubble" and reductions near the apex, each of which affect the electron temperature. We compare these results with satellite observations where applicable.

EQUIT-03 Three-Dimensional Modeling of Equatorial Spread-F Airglow Enhancements - by Jonathan Krall

Status of First Author: Non-student

Authors: J. Krall, J. D. Huba, and C. R. Martinis* Plasma Physics Division, Naval Research Laboratory, Washington, DC
*Center for Space Physics, Boston University, Boston, MA

Abstract: A sequence of 630.0 nm images obtained with the Boston University all-sky imaging system at Arecibo (18.3 N, 66.7 W, 28 N mag) shows equatorial spread-F (ESF) airglow depletions evolving into ESF airglow enhancements. Using a combination of a meridional wind and a converging zonal wind, the NRL ionosphere model SAMI3/ESF can reproduce ESF airglow enhancements. When ESF occurs in the presence of a steady, mild (20 m/s) meridional wind, the electron density in downwind “leg” of the geomagnetic field-aligned ESF plume can exceed the background density. Further, a mild (10 m/s) converging zonal wind pattern can disrupt the upward ExB motion of the plume, allowing the enhanced density to flow down to airglow-source altitudes. These results may also explain satellite observations of ESF density enhancements.

EQUIT-04 Ionospheric OI 630 nm Airglow Depletion Zonal Velocities over Ascension Island - by Narayan P. Chapagain

Status of First Author: Student IN poster competition PhD

Authors: Narayan P. Chapagain and Michael J. Taylor, Center for Atmospheric and Space Sciences, Utah State University, UT 84322, npchapagain@gmail.com

Abstract: We use 630 nm airglow image data from Ascension Island in the South Atlantic Ocean (7.9°S, 14.4°W, dip latitude 18.0 °S) measured by Utah State University all-sky imager during March 20 to April 7, 1997 to analyze ionospheric F-region plasma depletion zonal velocity. Airglow depletions were observed during 7 out of 17 nights, due to limited observing conditions. The velocities were typically 100-125 m/s during pre-midnight, decreasing during post-midnight in good accord with previous observations from other near-equatorial sites. However, on April 4-5 the normal eastward depletion motion was observed to reverse direction reaching speed up to 20 m/s over a 1.5 hour period around local midnight. During this reversal an unusual strong shear was observed with westward motion in the region which mapped to low apex altitudes (about 500-700 km) and eastward motion at higher apex altitudes (about 700-1200 km), with difference in the shear velocity up to 45 m/s. The westward reversal of the plasma bubbles probably resulted from a reversal in the F-region dynamo, or from a large increase in the altitude of the shear in the nighttime F-region plasma drift. These results will be compared with other recent studies.

EQUIT-05 On the possibility to infer ionospheric electric fields from the bottomside equatorial F-region irregularities - by Ronald Ilma

Status of First Author: Student IN poster competition PhD

Authors: Ronald R. Ilma and Michael C. Kelley, School of Electrical and Computer Engineering, Cornell University, Ithaca, NY

Abstract: Several studies have demonstrated that the backscatter from the so-called 150-km irregularities is a potential tracer of the F-region vertical drift. Similarly, the $E \times B$ plasma drift can be estimated from the ground magnetic signature at stations located off and under the influence of the equatorial electrojet. However, both methods uniquely provide reliable results during daytime hours. The aim of this work is to define a procedure to obtain ionospheric drift velocities from the plasma instability phenomena occurring in the bottomside of the equatorial F region. This would allow us to verify the concept by using data from the Jicamarca incoherent scatter radar. A subsequent step will be to find the one-to-one relationship between the layer time rate of altitude change and/or the Doppler shift of the irregularity in the bottomside F-region with the simultaneous incoherent scatter vertical drift measurements in the topside. Depending on the success of the expected result, the proposed method would be extended to the large database of JULIA radar observations, allowing the measurement of electric fields at times not accessible to the 150-km method. Further studies will include statistics of the scale size in bottom-type echoes and the role of seeding by the Kelvin-Helmholtz instability.

EQIT-06 Assimilative Modeling of Equatorial Plasma Depletions Observed by C/NOFS - by Yi-Jiun Su

Status of First Author: Non-student

Authors: Y.-J. Su,¹ J. M. Retterer,¹ O. de La Beaujardière,¹ W. J. Burke,^{1,2} P. A. Roddy,¹ R. F. Pfaff Jr.,³ G. R. Wilson,¹ and D. E. Hunton¹

¹Air Force Research Laboratory, Space Vehicles Directorate, Hanscom Air Force Base, MA

²Boston College Institute for Scientific Research, Chestnut Hill, MA

³Goddard Space Flight Center, National Aeronautics and Space Administration, Greenbelt, MD

Yi-Jiun.Su@hanscom.af.mil

Abstract: Using electric field measurements as drivers, the assimilative physics-based ionospheric model (PBMOD) reproduced density depletions observed at early morning local times during four consecutive orbits of the Communication/Navigation Outage Forecasting System (C/NOFS) satellite on 17 June 2008. However, the model's climatology-driven version that uses plasma drifts from empirical models predicted neither plasma depletions nor irregularities on this day. Coincident over flights of a large depletion by C/NOFS and the DMSP-F17 satellite allow estimates of its longitudinal and latitudinal scale sizes. The satellite-based estimates are shown to be in reasonable agreement with PBMOD predictions. The model's reproduction of observed temporal and spatial distributions of plasma depletions suggests that our assimilative technique can be used to enhance space-weather forecasts.

EQIT-07 Investigating Medium to Short Scale E-region Gradient Drift Waves Using Hybrid Simulations - by Yann Paul Tambouret

Status of First Author: Student IN poster competition PhD

Authors: Yann P. Tambouret, Meers Oppenheim, Center for Space Physics, Boston University

Abstract: Using massively parallel hybrid (kinetic ion, fluid electron) simulations, we investigate the growth of Gradient-Drift (GD) instabilities on the short to medium length scales. Radar observations of Type 1 and 2 echoes from E region plasma irregularities have been explained by the Farley-Buneman (FB) and GD instabilities. Linear theory argues that the FB mechanism produces primarily short wavelength instabilities while only long wavelengths (~1 km) are produced by the GD mechanism. A non-linear theory is necessary to account for radar measurements (limited to wavelengths <~15 m) of echoes made during ubiquitous GD-driving conditions. Ion kinetic effects are essential to accurately represent the short wavelength instabilities, but fully kinetic simulations are too expensive, particularly when resolving the long time and large spatial scales appropriate for the GD instability. We present a comparison of several hybrid techniques that allow us to run simulations with longer length scales and for longer times while capturing the necessary short wavelength physics. The kinetic ions are treated with a particle-in-cell algorithm. In one set of simulations, we use a standard 5-moment approximation to treat inertial electrons; in a second set, quasi-neutral and inertialess-electron approximations are made.

EQIT-08 Equatorial Spread-F in the Central Pacific: Seven Years of Airglow and Radar Data - by Ethan S Miller

Status of First Author: Student NOT in poster competition PhD

Authors: E. S. Miller, J. J. Makela (Illinois), R. T. Tsunoda (SRI)

Abstract: Equatorial plasma depletions have well-known seasonality and solar-cycle behavior. Except for a few well-instrumented sectors, much of these data have come from satellite sounding and in-situ observations. We present a climatology of optical airglow images and 50-MHz coherent backscatter from the Pacific sector from solar maximum (January 2002) to solar minimum (January 2009). In contrast to in-situ observations, we find that depletion activity remains quite high into solar minimum. However, the depletions and associated backscatter appear later in the evening and backscatter persists longer at solar minimum.

EQIT-09 Coincidence of Equatorial and Mid-Latitude Irregularities - by Ethan S Miller

Status of First Author: Student IN poster competition PhD

Authors: E. S. Miller, J. J. Makela (Illinois), R. T. Tsunoda (SRI)

Abstract: Alternating bands of light and dark, oriented in a NW-SE direction and propagating SW, are commonly observed in the 630.0-nm airglow over Arecibo and Hawaii, particularly during periods of low solar activity. The relationship of these structures to the familiar equatorial plasma depletions is not understood. We present several examples in the airglow over Hawaii and 50-MHz coherent backscatter from the Christmas Island radar showing the coexistence of equatorial and mid-latitude irregularities occurring simultaneously. While evidence exists that the mid-latitude structures are electrified (therefore mapping over the magnetic equator into the conjugate hemisphere) they are not often directly associated with coherent backscatter. We also present several case studies of this relationship.

EQIT-10 Studies of equatorial spread F using LISN VIPIR - by Gopi Krishna Seemala

Status of First Author: Non-student

Authors: S. Gopi Krishna¹, C.E. Valladares¹, P. Doherty¹, T. Bullet², R. Livingston³

¹ – Institute for Scientific Research, Boston College, St. Clement's Hall, 140 Commonwealth Ave, Chestnut Hill, MA - 02467, USA.

² – University of Colorado, Boulder, Colorado, USA

³ – Scion Associates, Port Townsend, WA, USA

Abstract: The Low latitude ionospheric sounding network (LISN) comprises of GPS receivers, VIPIR (ionosonde) and magnetometers deployed in South American region to study the dynamics of low latitude and equatorial ionosphere. The first VIPIR ionosonde has been installed and working temporarily in Jicamarca since October 2008. The VIPIR is able to operate in different modes; we have used high temporal and spatial resolution modes to measure the E and F regions. We carried out a campaign during March 2009 that aimed to measure the effect of gravity waves on the ionospheric densities and to observe the means of gravity waves as a seeding mechanism for spread F. This poster describes the preliminary results on the characteristics of ionospheric density structures, velocities during spread-F and sporadic-E conditions from the VIPIR data.

EQIT-11 Causal link of the wave-4 structures in plasma density and vertical plasma drift in the low-latitude ionosphere - by Tzu-Wei Fang

Status of First Author: Student IN poster competition PhD

Authors: T. W. Fang^{1, 2}, H. Kil³, G. Millward⁴, A. D. Richmond¹, J. Y. Liu², Seung-Jun Oh⁵

¹ High Altitude Observatory, National Center for Atmospheric Research, USA

² Institute of Space Science, National Central University, Taiwan

³ Johns Hopkins University, Applied Physics Laboratory, USA

⁴ Laboratory for Atmospheric and Space Physics, University of Colorado, USA

⁵ Space Environment Laboratory, Inc., Seoul, Korea

Abstract: We investigate the annual and local time variations of the wave-4 structures in the plasma density and vertical drift in the low-latitude F region by analyzing the measurements from the first Republic of China SATellite (ROCSAT-1) and conducting simulations with the Global Ionosphere and Plasmasphere (GIP) model. The GIP model uses a realistic magnetic field, neutral wind from HWM-07, and thermospheric parameters from the NRLMSISE-00 model. In order to understand how the vertical drifts relate to the longitudinal structure of the topside ionosphere, we apply the equatorial vertical drifts observed from ROCSAT-1 to drive the GIP model. The model well reproduces the longitudinal structure in electron density, and the magnitudes of electron density are comparable with ROCSAT-1 measurement at 600 km. The ROCSAT-1 observations of the vertical drift and plasma density show maximum amplitudes of their wave-4 components in July–September and minimum amplitudes in December–February. An eastward shift of the wave-4 components with increasing local time is observed both in the density and vertical drift. The GIP model density showed similar annual and local time variations of the wave-4 component. Since the model uses the observed equatorial vertical $E \times B$ drift as an

input, the results indicate the vertical drifts are essential in the formation and evolution of the longitudinal wave-4 density structure. The amplitude of the eastward propagating diurnal tide (DE3) at 110 km shows similar annual and local time variations as the F-region parameters, supporting the link between the DE3 tide, vertical $E \times B$ drift, and F-region plasma density on a global scale.

EQIT-12 The Thermospheric Midnight Temperature Maximum (MTM) As Seen in the Extended Whole Atmosphere Community Climate Model (WACCM-X) - by Joe McInerney

Status of First Author: Non-student

Authors: Joe McInerney and Hanli Liu, High Altitude Observatory(HAO), National Center for Atmospheric Research (NCAR)

Abstract: Many observation and modeling efforts have been made related to the thermospheric midnight temperature maximum (MTM) since it was first detected in the tropical upper thermosphere nearly 40 years ago. There have been a number of mechanisms suggested as the cause but there is still no clear explanation. Efforts to reproduce the MTM with global thermosphere models have been limited but a recent effort using the Whole Atmosphere Model (WAM) shows a more realistic model representation of the MTM. This prompted an effort to examine simulations from the recent extension of the Whole Atmosphere Community Climate Model (WACCM-X) for characteristics of the MTM. While this model is still undergoing development, especially the ionosphere component, it gives a reasonable representation of the thermosphere up to approximately 500 kilometers. Here we show characteristics of the MTM as it appears in WACCM-X and compare with previous observation and modeling results.

EQIT-13 C/NOFS Neutral Wind Meter Measurements of Neutral Thermospheric Helium Dominance at 400 km during Extreme Solar Minimum - by Robert Anthony Haaser

Status of First Author: Student IN poster competition PhD

Authors: R. A. Haaser, G. D. Earle and R. A. Heelis, W.B. Hanson Center for Space Sciences, University of Texas at Dallas, Richardson, Texas 75080

Abstract: From the middle of 2008 until now, solar activity has been unusually low, leading to a protracted solar minimum resulting in unusual atmospheric conditions, including the significant lowering of neutral Helium dominance cross-over which has been measured by CINDI instruments aboard the Communication/ Navigation Outage Forecast System (C/NOFS). The CINDI Neutral Wind Meter (NWM) aboard C/NOFS contains two instruments, the Ram Wind Sensor (RWS) and Cross Track Sensor (CTS) which can obtain velocity, temperature, composition and relative pressure information about neutral particles within the limits of the C/NOFS orbit altitudes (about the Earth), 402km – 850km. Due to the contracted thermosphere during the current solar minimum (analyzed from June to December 2008), the instruments, working at the edge of their pressure tolerances, have detected what appears to be a dominance of neutral Helium particles within the low orbital range of the satellite. It will be shown that this conclusion is supported by simultaneous measurements by the RWS and CTS instruments and is consistent with the measured mean drag on the satellite.

EQIT-14 Modeling the day-time eastward equatorial electric field - by Patrick Alken

Status of First Author: Student NOT in poster competition PhD

Authors: Patrick Alken, alken@colorado.edu, Stefan Maus, stefan.maus@noaa.gov, C. Manoj Nair, Manoj.C.Nair@noaa.gov

Abstract: The day-time eastward equatorial electric field (EEF) in the E-region plays an important role in equatorial ionospheric dynamics. It is responsible for driving the equatorial electrojet (EEJ) current system and the equatorial plasma fountain giving rise to the equatorial ionization anomaly (EIA). Due to the effects of the EIA on GPS navigation and radio wave communication, there is much interest in accurately measuring and modeling the EEF. In this work we use CHAMP satellite-derived latitudinal current profiles of the day-time EEJ in order to estimate the eastward electric field at all

longitudes, seasons, and day-side local times. We have constructed a dataset of over 36,000 individual EEF estimates based on six years of CHAMP data. This data was used to construct a climatological model of the EEF mean as a function of longitude, season, local-time, lunar local-time and solar flux level. Furthermore, we have created a model of the day-to-day variability of the EEF as a function of the same parameters. The climatological model EEFM can be obtained from <http://geomag.org/models/EEF.html>.

EQIT-15 Use of Incoherent Scatter Radar Data to Study the Equatorial Midnight Temperature Maximum (MTM) - by Christopher Miller

Status of First Author: Student IN poster competition Undergraduate

Authors: Christopher Miller, Electrical and Computing Engineering Department, Boston University
Carlos Martinis, Center for Space Physics, Boston University, William Oliver, Electrical and Computing Engineering Department, Boston university

Abstract: The midnight temperature maximum (MTM) is an enhancement of the neutral temperature T_n of ~ 50 -200 K in the nighttime equatorial thermosphere. This study will focus on the MTM feature using more than 100 days of ion temperature data obtained with Incoherent Scatter Radars (ISRs) at Arecibo and Jicamarca. The MTM will be characterized by fitting the data with a function that takes into account diurnal, semidiurnal and terdiurnal components; the time of MTM occurrence, the temporal duration, and the Temperature amplitude will be specified. Preliminary results are in agreement with general climatology of the MTM obtained with satellites and ground-based FPIs.

EQIT-16 The detection of a secondary peak in the nighttime measurements of thermospheric temperatures at Arequipa Peru (16.5S, 71.5 W) - by John W. Meriwether

Status of First Author: Non-student

Authors: J. W. Meriwether, M. Faivre, Department of Physics and Astronomy, Clemson University; R. T. Akmaev, T. Fuller-Rowell, F. Wu, NOAA Space Weather Prediction Center CIRES University of Colorado

Abstract: Fabry-Perot observations at Arequipa Peru have demonstrated the common occurrence of the midnight temperature maximum, which is a temperature increase of 100-200 K that is seen after midnight and before 04 local time during the months between March and October. Further examination of the nocturnal temperature data demonstrates the detection of an occasional secondary temperature maximum that is seen just after evening twilight between 20 and 22 LT. The amplitude of this feature is ~ 15 -20 K. Recent work using the Whole Atmosphere Model suggests that this secondary peak is a result of the upward propagation of a tidal wave integrating the effects of tidal harmonics (diurnal, semi-diurnal, terdiurnal,...) that interacts with the diurnal variation of plasma density to increase the thermospheric temperature during the early evening hours. This feature demonstrates the variability of the equatorial tidal structure of winds and temperatures that may impact the possible development and evolution of equatorial spread-F due to the variability of zonal winds caused by the tidal wave dissipating within the thermosphere.

EQIT-17 Inter-annual variability in the longitudinal structure of the low-latitude ionosphere due to the El-Nino Southern Oscillation - by Nicholas Pedatella

Status of First Author: Student NOT in poster competition PhD

Authors: Nicholas M. Pedatella, University of Colorado, Jeffrey M. Forbes, University of Colorado

Abstract: The ratio of monthly median foF2 values between the ionosondes at Maui and Yamagawa from January 1960 to June 1993 are used to investigate inter-annual variability in the wave-4 longitudinal structure of the low-latitude ionosphere. Analysis of Global Positioning System total electron content reveals that the ratio between these two locations is a suitable proxy for the amplitude of the wave-4 longitudinal structure in the northern hemisphere. Significant inter-annual variability is present in the foF2 ratio after removing the solar cycle and intra-annual variability. The remaining variability is thought to be due, in part, to changes in atmospheric and oceanic circulation arising from the El Nino Southern Oscillation(ENSO). Wavelet analysis reveals similar periodicities and occurrence time exists for the foF2 ratio monthly anomalies and sea surface temperature anomalies, represented by the Oceanic Nino Index (ONI). Furthermore, the yearly

ONI extreme value is well correlated with the extreme value of the foF2 ratio monthly anomalies in the subsequent five months. This surprising connection is attributed to changes in tropospheric convection associated with changing sea surface temperatures due to ENSO. This is thought to induce changes in the strength of the eastward propagating nonmigrating diurnal tide with zonal wavenumber $s = 3$ (DE3) which subsequently produces the observed changes in the wave-4 longitudinal structure. The results presented demonstrate that there is significant inter-annual variability in the ionospheric wave-4 longitudinal structure and further indicate that the ENSO phenomenon represents a source of ionospheric variability which has previously not been considered.

EQIT-18 Equatorial Zonal Electric Fields during the 2003 Sudden Stratospheric Warming Event - by Michael Enoch Olson

Status of First Author: Student NOT in poster competition PhD

Authors: Michael E. Olson and B. G. Fejer (Center for Atmospheric and Space Sciences, Utah State University, Logan, Utah, USA), J. L. Chau (Radio Observatorio de Jicamarca, Instituto Geofisico del Perú, Lima, Peru), C. Stolle (Deutsches GeoForschungsZentrum, Telegrafenberg, 14473 Potsdam, Germany), L. P. Goncharenko (Haystack Observatory, Massachusetts Institute of Technology, Westford, Massachusetts, USA)

Abstract: We use equatorial plasma drift and magnetometer observations from Jicamarca and magnetic field observations from the CHAMP satellite to study, for the first time, the temporal and spatial variations of equatorial ionospheric electric fields during the 2003 sudden stratospheric warming event. Our measurements illustrate the large and complex ionospheric response during this type of lower atmospheric perturbations.

EQIT-19 Estimation of ionospheric temperatures using Jicamarca IS radar data with beams pointed perpendicular to the geomagnetic field - by Pablo Martin Reyes

Status of First Author: Student IN poster competition Masters

Authors: Pablo Martin Reyes

Abstract: The availability of a new IS spectrum model for radar measurements perpendicular to the Earth's magnetic field by Milla and Kudeki [2009] is giving us the opportunity to revisit the problem of estimating F-region temperatures with the Jicamarca radar beam pointing in this direction.

In a typical perpendicular to B Jicamarca radar configuration, the antenna beam covers a range of magnetic aspect angles going from zero to about a degree, range in which the IS spectrum sharpens quite rapidly. Assuming that the state parameters of the ionosphere don't change for an observed region, the resulting spectrum will be the beam-weighted sum of the spectra, that only depends on the aspect angle. That way we get a forward model for the self- and cross-spectrum between the north and south quarters of the Jicamarca array configured as an interferometer. We are showing here the modeling of the beam-weighted IS spectrum and cross-spectrum, and the estimation of the temperatures from data taken with the Jicamarca IS radar.

EQIT-20 Estimating Model Parameters from Ionospheric Reverse Engineering by Seebany Datta-Burua

Status of First Author: Non-student

Authors: Seebany Datta-Barua, Gary Bust, and Geoff Crowley

Abstract: Several active areas of ionospheric research, such as storm-enhanced densities, require knowledge of physical drivers. Ideally, we would like to have direct global measurements of the winds, electric fields, composition, and temperatures: the drivers of the ion continuity equation. However, in practice, there are so few ground-based instruments and satellites measuring these parameters that knowledge of the drivers is usually missing. On the other hand, the ready availability of ground-based GPS total electron content (TEC) and other ionospheric data has allowed imaging algorithms such as the Ionospheric Data Assimilation Three-Dimensional (IDA4D) [Bust et al., 2000, 2004] to routinely obtain images of the global electron density field with spatial resolution of 100 kilometers horizontally and 20 kilometers vertically. We

investigate whether these images can be inverted to provide information about the physical drivers such as electric fields and winds.

We are developing a new inversion algorithm, based on 4D images of global electron density, to estimate ionospheric driver when direct measurement is not available. Previous studies on simulated data from TIMEGCM showed that the field-aligned neutral wind could be estimated to within about 30% of the simulated “true” winds [Datta-Barua et al., in press]. We begin with a model of the ion continuity equation that includes production and loss rate estimates for the F region. We use ion and electron temperatures from IRI and neutral species temperatures and densities from MSIS, for estimating the magnitude of these effects. We then model the ExB drift and neutral wind as a power series at a given longitude for a range of latitudes and altitudes. To test our algorithm, we input IDA4D electron densities, estimate the field-aligned and field-perpendicular electron speed at 15-minute intervals, and validate by comparing to measured field-aligned and field-perpendicular electron velocities from the Arecibo Incoherent Scatter Radar (ISR).

We show results for a storm day: 10 November 2004. The agreement between the velocities derived from IDA4D versus Arecibo true velocities appears to be stronger during periods of enhanced speeds. This is to be expected, since during these times, they are the dominant processes. Despite the potential temporal and spatial limits on accuracy, estimating drifts from measured electron density fields provided by IDA4D via our algorithm shows great promise as a complement to the more sparse radar and satellite measurements.

EQIT-21 Non-specular meteor measurements of lower thermosphere winds - by Glenn Sugar

Status of First Author: Student IN poster competition Undergraduate

Authors: Glenn Sugar, gsugar@bu.edu, Meers M. Oppenheim, Nicholas O. Slowey, Elizabeth Bass, Jorge L. Chau, Sigrid Close

Abstract: Current methods used to measure lower thermosphere winds are either difficult and costly, or fail to provide detailed altitude resolution. Rocket experiments designed to measure these winds cost on the order of a million dollars, while specular meteor radars cannot give resolution better than 1 km. Oppenheim et al., 2009 describe a new method to measure these winds using non-specular meteor trail echoes. A radar with interferometry pointing nearly perpendicular to the geomagnetic field can observe and track non-specular trails as they are blown by the neutral winds. This poster presents the first time evolution of wind profiles using this new technique with data from the Jicamarca Radio Observatory. The wind profiles observed show winds as fast as 150 m/s as well as significant wind shears. These observations span 90 km to 110 km altitude with a resolution of 75 meters. We examine the change in the winds over the course of three hours. The non-specular meteor method is far less costly than rocket campaigns while providing detailed range resolutions. Further refinement of the experiments and analysis will provide an inexpensive, reliable, and practical method to monitor the lower thermosphere winds.

Long-Term Variations of the Upper Atmosphere

LTRV-01 Long Term Monitoring of Geocoronal Hydrogen - by Susan Nossal

Status of First Author: Non-student

Authors: S.M. Nossal, E.J. Mierkiewicz, F.L. Roesler, L. M. Haffner, R.J. Reynolds, R.C. Woodward
University of Wisconsin-Madison
University of Wisconsin-Fond du Lac

Abstract: The Wisconsin long-term data record of Northern hemisphere mid-latitude geocoronal Balmer-alpha emissions now spans more than two solar cycles. Hydrogen is a primary constituent of the neutral atmosphere and is a byproduct of radiatively important species below such as methane and water vapor. We will discuss the Wisconsin long-term Balmer-alpha emission data record, methods of error assessment, and modeling studies of the solar cycle variation. We use the LYAO_RT radiative transfer code of Bishop [1999, 2001] to extend to exospheric altitudes and to compare the observed Balmer-alpha intensities with those calculated using the hydrogen density distribution in the Mass-Spectrometer-Incoherent-Scatter model. The MSIS distribution yields a solar maximum to minimum trend similar to that observed; however there are significant differences in magnitude between predicted and observed intensities.

LTRV-02 Climatology of the antiparallel plasma drift over Arecibo Observatory - by Eva Robles

Status of First Author: Non-student

Authors: Christiano Garnett Marques Brum, 1Pedrina Terra, 1Sixto Gonzalez, 1Nestor Aponte and 1Craig Tepley; 1-National Astronomy and Ionosphere Center, Arecibo Observatory, Puerto Rico

Abstract: In order to study the long trend variation of the neutral winds registered over Arecibo, we are analyzing the responses of the antiparallel plasma drift velocity at the peak of the ionosphere (hmF2) to the variations of solar and geomagnetic activity, and its dependence in time and season. From 1985 through 2004, there were 243 nights of Incoherent Scatter Radar (ISR) data analyzed.

Midlatitude Ionosphere or Thermosphere

MDIT-01 Topside ionosphere responses to a moderate geomagnetic storm - by Diana C Prado

Status of First Author: Student IN poster competition Undergraduate

Authors: Diana Prado, Christiano Brum, Sixto Gonzalez, Nestor Aponte, Ezequiel Echer

Abstract: We are analyzing the responses of the topside ionosphere parameters to the geomagnetic storm. For this purpose we chose the period from March 7 – March 11, 2008. This was a complex magnetic storm with a main phase decrease being non-monotonic presenting three decreases (or dips). The recovery phase was also complex with a secondary Dst index decrease. The topside ionosphere data used was registered by the Incoherent scatter radar (ISR) of the Arecibo Observatory. The Arecibo radar is extremely powerful and sensitive and it is capable of making very accurate measurements of many ionospheric parameters. In this work, data analysis was performed with H⁺, O⁺ and He⁺ ion concentrations, electron density, and ion and electron temperatures. These records display radar data from twenty eight different altitudes (224 to 1248km of altitude with step of the \square 38km) with an acquisition rate of about twenty minutes. Previous results show an increase of almost two orders of the electron densities and electron and ion temperatures at 641km of altitude. In the same height the O⁺ fraction decreased and a slight increase of the H⁺ concentrations was observed.

MDIT-02 Numerical simulation and observational study of ion layer formation at Arecibo by Yun Gong

Status of First Author: Student IN poster competition Masters

Authors: Yun Gong, Qihou Zhou, Y. T. Morton

Abstract: Ion layer formation is a manifestation of the complex physical and chemical processes in the ionosphere. This study explores how tidal winds, ambipolar diffusion, meteoric ablation and lower ionospheric chemistry contribute to the vertical transport. Here, we develop a one-dimensional model to understand the time-dependent vertical distributions of metallic ions from 80 to 150 km. This is the first time that the ambipolar diffusion velocity has been included. The effect of ambipolar diffusion is to largely wipe out the formation of thin layers above 120 km and broaden the layer width below 120 km. Furthermore, we represent the layer trajectory and layer width results from Arecibo incoherent scatter radar data. Key words: Ambipolar diffusion, Tidal winds, Convergence of metallic ions

MDIT-03 Quiet time Latitudinal Variations of Ion drifts in the Ionosphere at Low- and Middle Latitudes - by Edgardo Pacheco

Status of First Author: Student IN poster competition PhD

Authors: Edgardo Pacheco, Roderick Heelis, S-Y. Su

Abstract: We provides a global description of meridional and zonal ExB ion drifts at low and middle latitudes that are key elements for the understanding of the dynamics of the ionosphere and are important parameters for physics-based models.

We use measurements from the ROCSAT-1 satellite for the years 1999-2003 taken at altitudes near 600 km. Offsets in the original data are removed by considering separately the northbound and southbound passes in a given volume, and enforcing magnetic conjugacy for the ion drift components perpendicular to the magnetic field. Our study investigates latitudinal, longitudinal and local time variations of ion drifts in the topside ionosphere for the geographic latitude range from -25° to $+25^{\circ}$. Specifically, we derive the ion drifts in the direction perpendicular to the magnetic field during quiet times defined when the Dst index is greater than -100 nT and the Kp index is equal to or less than 3. We then describe the longitudinal differences in the latitude and local time profiles of the ion drifts for different seasons.

MDIT-04 Analysis of Arecibo dual beam world day data from 2006 to present – Results from the weakest solar minimum since 1928 - by Edvier Cabassa-Miranda

Status of First Author: Student IN poster competition Undergraduate

Authors: 1Edvier Cabassa-Miranda, 1Diana Prado Garzón, 1Ali Amirrezvani, 2Diana Centeno, 2Eframir Franco, 3Aleshka Carrion, 3Cristina Padilla, Mike Sulzer, Christiano Brum, Nestor Aponte, Sixto A. González
All- National Astronomy and Ionosphere Center, Arecibo Observatory, Puerto Rico
1-University of Puerto Rico, Mayagüez Campus
2-University of Puerto Rico, Humacao Campus
3-University of Puerto Rico, Rio Piedras Campus

Abstract: In this work we are presenting the climatology of the F region obtained by the Arecibo dual beam world day data from 2006 to present. This period represents the weakest solar minimum since 1928. For this propose, 67 days of data were reduced and separed by season and geomagnetic activity and compared with data of the earlier solar minimums (22 and 23 cycles) under same areonomic conditions. In order to study their variability with geomagnetic activity, we are comparing with kp index. Previous results of the earliest solar minimums show that the dependence with geomagnetic activity appears of different ways with the seasons and time, with major variations in the hmF2 parameters at nighttime before the midnight local time. Also, we found a increase of the electron density from 1985 to 2005 in the peak of F region and the altitude of the hmF2 suffered a decrease of ~ 0.74 km year.

MDIT-05 Ionospheric variations during January 2009 stratospheric sudden warming by Larisa Goncharenko

Status of First Author: Non-student

Authors: L. Goncharenko, A. Coster, W. Rideout, J. Chau, C.E. Valladares, H. Liu

Abstract: The stratospheric sudden warming peaking in January 2009 was the strongest and most prolonged on record. We report significant ionospheric variations is association with this event, which are especially pronounced at low latitudes. Large increase in the vertical drifts is observed at Jicamarca, displaying 12-hour signature with upward drifts in the morning hours and downward drifts in the afternoon hours, with pattern persisting for several days. Analysis of GPS TEC data indicates that variations in electron density are observed in a large range of longitudes and latitudes. The entire daytime ionosphere is affected, with morning increase in low-latitude TEC exceeding 100% of the mean value, and afternoon decrease in TEC approaching $\sim 50\%$ of the mean value. These variations are consistent with ionospheric disturbances observed during other stratospheric warming events. We suggest the observed phenomena is related to planetary waves, which have a high amplitude level prior to the stratospheric warmings. Interaction of planetary waves with tides and modulation of tides can lead to changes in the low-latitude electric field through the wind dynamo process, which in turn is responsible for a large-scale redistribution of ionospheric electron density.

MDIT-06 Joint FPI/ISR Observations at Millstone Hill Observatory - by Larisa Goncharenko

Status of First Author: Non-student

Authors: L. Goncharenko, P. Erickson, J. Noto, J.R. Riccobono, S. Kapali, and M.A. Migliozzi

Abstract: A 100mm diameter Fabry-Perot Interferometer (FPI) has been operating at the Millstone Hill Optical Laboratory since April, 2009. This single-etalon instrument makes measurements of the 6300\AA airglow emission every night, except

during full moon periods. This new FPI provides neutral temperature and winds just below the F2 ionospheric peak. The instrument uses 10.525mm etalon spacing and an Andor DW 436 camera with a 2048 X 2048 pixel E2V Technologies thinned and back-illuminated array detector. The CCD quantum efficiency is approximately 60% at 6300Å. Four FPI orders are simultaneously sampled over a field of view of 2.8 degrees. Ring summing and spectral analysis software accompanies the system and is available to all users. Winds are derived by measuring the line-center Doppler shift (relative to zenith) in the cardinal compass directions, and pointing is achieved with a mirror system that operates beneath a Plexiglas dome. The system can be operated remotely with the data taking software, including pointing and wavelength calibration. This instrument continues the red-line database from Millstone Hill that began more than 30 years ago, with a 30-fold sensitivity improvement over the configuration used prior to 2009.

We present first observations from the FPI and compare them to the simultaneous data obtained by the Millstone Hill incoherent scatter radar during the joint experiment of Apr 23-24, 2009. To discuss observed signatures in context of seasonal change and solar minimum conditions, we also compare these observations to average patterns observed by Millstone Hill ISR during the current and prior solar minimums.

MDIT-07 COSMIC Observations of TEC Enhancements during Magnetic Disturbances by Peichen Lai

Status of First Author: Student IN poster competition PhD

Authors: Peichen Lai, Chin S. Lin and William J. Burke

Abstract: COSMIC satellite data, acquired in May and December 2007 were analyzed to study TEC enhancements. GPS signals detected by COSMIC satellites were inverted via radio occultation techniques to obtain vertical electron density profiles. We then calculated Total Electron Content (TEC) by integrating electron density profiles over altitude. Locations assigned to TEC values are at ray tangent points. Obvious TEC enhancements appear at high magnetic latitudes during storm periods, with observed increases sometimes exceeding background values by factors of 3 to 4 during disturbed period. The strongest TEC intensifications were found at sub-cusp latitudes in the local noon sector. Thermospheric-wind and Appleton anomaly effects show up at middle and low magnetic latitudes. Dependencies of TEC enhancements on magnetic local time, magnetic latitude, and storm phase will be presented. Possible relations between ionization patches at high magnetic latitudes near local noon and plasma drainage plumes will also be discussed.

MDIT-08 The Properties and 3D Structure of Medium Scale Traveling Ionospheric Disturbances - by Ilgin Seker

Status of First Author: Student IN poster competition PhD

Authors: Ilgin Seker (ilgins@psu.edu), John D. Mathews (JDMathews@psu.edu), The Pennsylvania State University

Abstract: Perhaps the most persistent and prominent of the mid-latitude phenomena is the Medium-Scale Traveling Ionospheric Disturbances (MSTIDs) in the F-region. These MSTIDs have been given various other names such as plasma depletion bands, plasma bubbles, ionospheric slabs, and thermospheric waves. Using imager and radar together to observe these MSTIDs proves to be very useful. In particular, the plasma structures seen in the narrow-beam, azimuth-scanning incoherent scatter radar (ISR) results cannot be understood fully without the allsky images which provide the horizontal context for the vertical radar results. Important results on the 3D geometry of these structures are found using a specific observation technique that is based on the combined ISR and allsky imager observations of MSTID structures in the F-region over the Arecibo Observatory (AO) in Puerto Rico. For the first time, it is shown that the southern part of an MSTID band reaches higher altitudes than its northern part meaning that the MSTID bands are vertically tilted. In order to further confirm these findings, a 3D empirical model of MSTID bands based on these observations is constructed. This empirical model is intended to replicate both the azimuth-scanning ISR and the allsky imager results, and is especially useful in explaining how these complex structures appear in azimuth-scanning ISR results. ISR and allsky imager results derived from the model are compared with the actual observations, and important findings are highlighted. The results give a much broader perspective on nighttime, mid-latitude F-region and point to new ways of interpreting MSTID structures and how they appear in ISR results. Furthermore, the results of the empirical model provide clues on what to expect from the theoretical models of geomagnetically quiet, nighttime, mid-latitude, F-region electrodynamics.

MDIT-09 Three-dimensional simulation of the coupled Perkins and Es layer instabilities in the nighttime midlatitude ionosphere - by Tatsuhiro Yokoyama

Status of First Author: Non-student

Authors: Tatsuhiro Yokoyama(1), David L. Hysell(1), Yuichi Otsuka(2), Mamoru Yamamoto(3)

1. Department of Earth and Atmospheric Sciences, Cornell University, Ithaca, NY, USA
2. Solar-Terrestrial Environment Laboratory, Nagoya University, Nagoya, Japan
3. Research Institute for Sustainable Humanosphere, Kyoto University, Uji, Japan

Abstract: Plasma density structures and associated irregularities in the nighttime midlatitude ionosphere are frequently observed as frontal structures elongated from northwest to southeast (NW-SE) in the northern hemisphere. The frontal structures and the coupling process between the E and F regions are studied with a three-dimensional numerical model which can simulate two instability mechanisms: Perkins instability in the F region and sporadic-E (Es)-layer instability in the E region. The fastest growth of the coupled instability occurs when the unstable conditions on NW-SE perturbation are satisfied in both regions. The perturbation of F-region integrated conductivity grows much faster than the isolated Perkins instability. The meridional component of a rotational wind shear blows an existing Es layer southward, and the F-region structure follows the E-region drift velocity. NW-SE structure in the E region can be formed from random perturbation regardless of the F-region condition. When the F region is unstable on the NW-SE perturbation, however, the NW-SE structure is formed in both regions with a common scale length. We conclude that (1) the Es-layer instability plays a major role in seeding NW-SE structure in the F region, and the Perkins instability is required to amplify its perturbation, (2) the rotational wind shear in the E region produces southwestward phase propagation of the NW-SE structure in both the E and F regions, and (3) the coupling process has a significant effect on the scale of the Es-layer perturbation rather than the growth rate of the Es-layer instability.

MDIT-10 Tool for the Assessment of Ionospheric Models - by Jonathan V Thompson

Status of First Author: Student IN poster competition Undergraduate

Authors: Jonathan Thompson, Vince Eccles, Jan Sojka, Space Environment Corporation, Providence, UT, Hien Vo, Sixto Gonzalez, Arecibo Observatory, Arecibo, Puerto Rico

Abstract: The ionospheric F-region is a dense layer of free electrons and ions in the upper atmosphere (200 to 1000km). The day to day characteristics of the ionosphere can affect modern GPS navigation and communications technologies. To mitigate ionospheric effect on these technologies, we require greater accuracy in the electron densities generated by ionospheric models. Models, both empirical and physical, have been developed to increase our understanding of the ionosphere and to predict its characteristics. The Arecibo Radar Observatory provides approximately 700 days of data concerning the F region spanning 50 years and 4 solar cycles. We have collected, reduced, and cleaned the Arecibo Radar electron density observations to create our “ground-truth database”. By using the Arecibo data and the 1991 International Reference Ionosphere(IRI12) as a standard for comparison, we are able to provide an assessment of ionospheric models. This assessment is based on metrics and skill scores over several ionospheric profile parameters: peak density values, peak density altitudes, and the shape of the electron density profile with altitude. The results of this assessment will greatly assist us in improving current models of the ionosphere.

MDIT-11 Midlatitude Observations of the Thermosphere Implementing a Fabry-Pérot Interferometer - by Gregory Twork

Status of First Author: Student IN poster competition Undergraduate

Authors: Gregory Twork

Abstract: The Pisgah Astronomical Research Institute (PARI) is a non-profit public foundation that collaborates with several universities, with the purpose of providing an educational and research opportunities in the many fields of science. On July 11, 2007 at PARI Clemson University installed a Fabry-Pérot interferometer (FPI) which uses a series of reflective surfaces and focusing lenses to produce a circular diffraction pattern from the 630nm emission of atomic oxygen. These diffraction rings are then analyzed based on peak width and intensity. As these parameters change, the Doppler shifts and

Doppler broadenings give information about the upper atmosphere winds and temperatures. This interferometer will be used in conjunction with another Fabry-Pérot located in Arequipa, Peru to observe these oxygen emissions in order to study the Midnight Temperature Maximum (MTM), a nighttime thermal event occurring in the equatorial thermosphere. The interferometer located at PARI will eventually be used not only as an experimental station, but also as an educational tool.

MDIT-12 SOFDI/CASI Observations of the September 2005 Storm - by Russell B Hedden

Status of First Author: Student IN poster competition PhD

Authors: Russell B Hedden

Abstract: The Second Generation Optimized Fabry Perot Doppler Imager (SOFDI), a state-of-the-art triple-etalon Fabry Perot interferometer capable of making day and night wind and temperature measurements, is soon to be deployed to Huancayo, Peru along with the Cornell all-sky imager (CASI) in support of the C/NOFS satellite. We present an overview of the contribution SOFDI and CASI will make by presenting nighttime results of 630-nm OI emission observations taken in upstate New York during the September 2005 storm period.

MDIT-13 Multi Line Investigations of the Hydrogen Geocorona - by Elise K. Larson, presented by Edwin Mierciewicz

Status of First Author: Student NOT in poster competition Undergraduate

Authors: E. K. Larson, E. J. Mierkiewicz, F. L. Roesler, L. M. Haffner, S. M. Nossal

Abstract: Studies involving the hydrogen Balmer-alpha and Balmer-beta emissions in the geocorona, or the Earth's uppermost atmosphere, are leading towards greater understanding of the characteristics, chemistry, and variability of the geocorona. These emission line studies will help to refine modeling techniques used in geocoronal analysis. In particular, the Balmer-beta emissions have not been extensively studied, and therefore provide added insight through their relationship to the Balmer-alpha emissions. In this poster we will explore this relationship, presenting new data on the variation in the emissions with shadow altitude and time of night. This research is an important first step in the retrieval of hydrogen densities from ground-based Balmer series emissions.

MDIT-14 Impulse-like increase of the nightglow [OI] 630 nm line intensity and its possible reason as a shear excited atmospheric vortical perturbations - by Goderdzi Didebulidze, presented by Nikoloz Gudaze

Status of First Author: Non-student

Authors: G. G. Didebulidze; L. N. Lomidze; N. B. Gudadze; M. Todua

Abstract: The wave-like disturbances (with duration about 1-3 hours) in the mid-latitude total nightglow intensity of the oxygen red 630.0 nm line observed at Abastumani (41.75oN, 42.82oN) are shown. The observed impulse-like increase of the red line intensity followed by oscillations, characteristic for short-period atmospheric gravity waves (AGWs), is considered as a possible result of transformation of shear excited three-dimensional vortical perturbation (shear wave) into AGW. The shear wave can produce an enhancement of the northward wind (or decrease in the southward one), which can cause a downward motion of the F2 layer peak height resulting in the impulse-like increase in the red line intensity. The theoretical explanation of this phenomenon is based on the time dependent simple Chapman-type layer taking into account the presence of AGWs and meridional wind field reversal. The possibility of the impulse-like increase in the red line intensity under the influence of shear excited waves with vertical wave-number $kz \neq 0$ is demonstrated analytically and numerically.

MDIT-15 Prompt Penetration of the Interplanetary Electric Field to the Mid Latitude Ionosphere - by Yan Yin

Status of First Author: Student NOT in poster competition PhD

Authors: Yan Yin, yinyan@vt.edu, Jo Baker and Mike Ruohoniemi, jo.baker@vt.edu mikeruo@vt.edu, Department of Electrical and Computer Engineering, Virginia Tech

Abstract: Research on prompt penetration of interplanetary electric field to the mid and low latitude ionosphere dates back to the 1968. However, there are still controversies on shielding the details of the penetration, in particular, the time scales on which it operates. SuperDARN radars with high time resolution and range resolution observe the ionosphere continuously. With the help of this radar network, especially the newer mid-latitude radars, we are able to look deep into the details of shielding and measure penetration timescales. We focus on the undershielding situation for prompt electric field penetration into the mid latitude ionosphere. A review of interplanetary magnetic field (IMF) Bz data of 2008 produced 95 events with steady positive IMF Bz for more than 30 minutes followed by steady negative Bz for more than 30 minutes with a quick transition between them. We reviewed these events and found that there are more than 20 events having velocity enhancements measured by SuperDARN that can be related to the IMF Bz southward turnings. In addition, there were more than 20 other events that exhibited other phenomena that can be related to southward turnings of IMF Bz, such as backscatter power enhancement and backscatter range gate increase. Based on review of these events, we characterize the ionosphere irregularities during prompt undershielding penetrations, establish timescales of penetration for undershielding events and describe plasma movements in the F region during undershielding events.

Polar Aeronomy

POLA-01 Preliminary Results from the CASCADES-2 Sounding Rocket - by Erik Thomas Lundberg

Status of First Author: Student IN poster competition PhD

Authors: Erik Lundberg, Paul Kintner, Cornell University, Kristina Lynch, Meghan Mella, Dartmouth College, Marc Lessard, University of New Hampshire

Abstract: At 11:04:00 UT on March 20th, the high altitude auroral sounding rocket CASCADES-2 was launched from Poker Flat Research Range (PFRR) into a Poleward Boundary Intensification (PBI). Prior to reaching an apogee of 564km the payload split apart into 5 instrumented subpayloads. Two electric/magnetic field payloads consisting of 12m tip-to-tip wire booms are ejected at a high velocity parallel to the magnetic field, achieving a separation distance of 8km. Two small payloads consisting of electron detectors are ejected perpendicular to the magnetic field from the main payload which carries electron and ion detectors. On the downleg of the flight the rocket encountered a number of interesting phenomena including, auroral hiss, BBELF waves, upper hybrid waves, electron plasma waves, and intense Alfvénic fluctuations in excess of 200mV/m. Preliminary results from these field and particle instruments are presented.

POLA-02 Dynamic variability in ionospheric composition at high latitudes - by Matthew Zettergren

Status of First Author: Student NOT in poster competition PhD

Authors: M. Zettergren, J. Semeter, C. Heinselman, M. Diaz, P-L. Blelly, M. Diaz, B. Burnett

Abstract: Incoherent scatter radar (ISR) is a powerful remote sensing tool for probing the high-latitude ionosphere. Spectral analysis of radio waves scattered from the ionosphere allows for the simultaneous determination of several important plasma state parameters as a function of range. In almost all cases, the relative concentrations of molecular and atomic ions must be assumed in order to extract ion and electron temperatures from the spectra. However, theoretical models have shown that strong electric fields change ion composition dramatically in the F-region due to enhanced frictional heating which affects chemical reaction rates. Changes in ion composition due to this process are likely to violate assumptions of static composition made in standard ISR spectral analysis.

This study presents a new method to estimate ion composition from ISR measurements. Ion temperature/mass ambiguities are mitigated by using a model of ion frictional heating to self-consistently constrain the ion temperature profile and allow

the spectra to be fitted for ion composition. This method is applied to several sample data sets. Results are shown to be consistent with theoretical model calculations and also demonstrate typical characteristics of molecular ion enhancements due to frictional heating.

POLA-03 Measurement of E-region neutral winds with the Poker Flat all-sky imaging Fabry-Perot spectrometer - by Carl Andersen

Status of First Author: Student IN poster competition Masters

Authors: Carl Andersen, University of Alaska Fairbanks and Mark Conde, University of Alaska Fairbanks

Abstract: The all-sky imaging Fabry-Perot spectrometer located at Poker Flat, Alaska is capable of obtaining measurements of the horizontal neutral wind field via 5577 Å [O I] aurora/airglow emission. Two difficulties which arise in measuring neutral winds with the green line are discussed. The first issue is a result of chromatic aberration specific to the Poker Flat FPS. The second is the caused by the variability of the altitude at which green line emissions occur. Some examples from the 2002-2004 observing campaign are presented. One common feature in the data collected so far is a strong response of the neutral wind on short spatial and temporal scales to auroral activity.

POLA-04 Estimation of vector velocity field using an array of spatially distributed ISR measurements - by Thomas Butler

Status of First Author: Student NOT in poster competition PhD

Authors: T. Butler, J. Semeter, C. Heinselman, M. Nicolls

Abstract: We explore a technique for reconstructing flow fields from ISR measurements in the ionospheric F-region. This study uses measurements obtained at the Poker Flat Incoherent Scatter Radar (PFISR) in Alaska. Using PFISR's ability to steer the beam pulse-by-pulse, we acquire essentially simultaneous measurements in an array of 26 beam directions arranged in a 5 x 5 grid with one additional beam in the up-B direction. Bulk plasma drift results in a Doppler shift of the spectrum of the observed signal. This permits observation of the component of the drift velocity in the line-of-sight of the radar. By combining adjacent measurements of this type, it is possible to resolve vector velocity. We analyze the limitations of this type of reconstruction and show an example using data from a March 2009 experiment.

POLA-05 The role of k_{\parallel} on wave heating in the auroral E region - by Gabriel Percy Michhue

Status of First Author: Student IN poster competition PhD

Authors: G. Michhue (1), D. Hysell (1)

1. Department of Earth and Atmospheric Sciences, Cornell University, Ithaca, NY, USA

Abstract: For many years, incoherent backscatter radars observations at high latitudes have shown strong electron temperature (T_e) enhancements in the E-region correlated with the convection electric field (E_c). It is accepted now that the mechanism responsible for the enhancements involves Farley-Buneman (FB) waves.

Extending a linear theory of FB instability and following a quasi-linear approach in this work, we propose a model that predicts electron and ion temperature enhancements for a given external convection electric field.

For a given E_c and using the FB dispersion relationship, we find the flow angle (k_{\parallel}/k) that gives marginal instability, and following Dimant and Milik's model, a corresponding heat source is included in the longitudinal heat transport equation. After solved this equation, a new T_e is introduced in the dispersion relationship iteratively until a stationary T_e is found.

POLA-06 Numerical Estimates of Polar Cusp Neutral Upwelling Using Satellite Conjunction Data - by Brent Sadler

Status of First Author: Student IN poster competition PhD

Authors: F. Brent Sadler, Marc R. Lessard, Eric Lund, H. Luhr, G. Crowley, A. Otto

Abstract: Recent observations have confirmed neutral particle upwelling at high latitudes which are localized to the polar cusp region and seem to be correlated to high auroral activity. For decades, thermospheric upwelling has been recognized as an important topic and has been studied observationally and theoretically, with efforts largely focused on Joule heating being the basic driver. As data and models have improved over the years, Joule heating has indeed proven to be fundamental to upwelling, at least at lower altitudes. At higher latitudes, however, the situation appears to be more complex and recent results indicate that Joule heating alone is not adequate. We investigate this issue with numerical models using data acquired by FAST and CHAMP satellites. Field and particle data from FAST and accelerometer data CHAMP are used from a single favorable conjunction alignment event. We compare results from two different models: a Joule heating model ("thermodynamic") and an auroral precipitation model (electrodynamic).

POLA-07 Double Probe Electric Field Measurements - by Erik Stromberg

Status of First Author: Student IN poster competition Undergraduate

Authors: Erik Stromberg

Abstract: The energy input into the upper atmosphere at high latitudes varies both temporally and spatially over the Earth's Polar Regions. This is due to changing solar wind conditions and the resulting interactions with the Earth's magnetosphere that couples energy to the upper atmosphere. The electric field is the key indicator of the amount of heating occurring in these upper atmospheric regions. Obtaining electric field measurements at high spatial and temporal resolution in the high-latitude regions is critical to our understanding of and our ability to predict the state of the space environment. The necessary electric field measurements could be obtained in-situ using a constellation of satellites distributed in different orbits each with electric field double probes. An affordable constellation could be constructed using CubeSats each with crossed wire booms that extend into the plasma environment from opposite sides of the spacecraft. Although there are several technical challenges to constructing such a constellation, one of the first is developing a suitable miniature wire boom system for an electric field instrument that can be accommodated on a CubeSat. We present a design for a 10 meter tip-to-tip wire boom system to deploy four 1-cm spherical double probe sensors from a CubeSat. The wire boom mechanism consists of a wire spool which is controlled with a small non-magnetic, piezoelectric motor, to control the deployment of the booms from a spinning CubeSat. The wire boom system will take up no more than a 1.25cm high slice through a standard 10x10cm CubeSat cross section. The current design is less than 30 grams in weight and will not draw more than 0.1 Watts (.6 peak) power during active deployment. This wire boom system is being developed by a team of USU students in the College of Engineering at Utah State University with support from the Space Dynamics Lab. The spherical sensors at the end of the wire booms will be gold plated to minimize geometric work function dissimilarities and to provide surface electrical stability. The proposed crossed probes design permits the measurement of the two-dimensional electric field at a fixed spatial scale determined only by the spacecraft velocity and the instrument sampling rate.

Alken, Patrick, 22
Andersen, Carl, 32

Bayne, Stephen, 9
Burnett, Benjamin, 7
Bust, Gary, 8
Butler, Thomas, 32

Cabassa-Miranda, Edvier, 27
Chandrasekran, Priyanka, 16
Chapagain, Narayan, 19

Datta-Burua, Seebany, 24
Davidson, Ryan, 10
De La Jara, Cesar, 11
Didebulidze, Goderdzi, 30
Drake, Kelly, 1

Emery, Barbara, 1

Fang, Tzu-Wei, 21
Fedrizzi, Mariangel, 3

Gallagher, Hugh, 8
Garner, Trevor, 9
Gerhardt, David, 1
Goncharenko, Larisa, 27
Gong, Yun, 26

Haaser, Robert, 22
Hackett, Alexander, 7
Hedden, Russell, 30
Hibit, Eli, 8
Huang, Yiyi, 16

Ilma, Ronald, 19

Joyce, Glenn, 18

Kalogerakis, Konstantinos, 10
Knipp, Delores, 3
Kor, Sandeep, 15
Krall, Jonathan, 19

Lai, Peichen, 28
Larson, Elise, 30
Lin, Chin, 4
Liu, Xianjing, 5
Luan, Xiaoli, 4
Lundberg, Erik, 31

Mahrous, Ayman, 9
Matsuo, Tomoko, 5
Matteo, Nick, 16
McInerney, Joe, 22
Meriwether, John, 23
Michhue, Gabriel, 32
Miller, Christopher, 23
Miller, Ethan, 20, 21
Minin, Serge, 7

Nikoukar, Romina, 13
Nishioka, Michi, 18
Nossal, Susan, 25

O'Hanlon, Brady, 11
Olson, Michael, 24

Pacheco, Edgardo, 26
Parris, Richard, 12
Pawlowski, David, 2
Pedatella, Nicholas, 23
Pettigrew, Ellen, 3
Pilinski, Marcin, 13
Prado, Diana, 26

Reyes, Pablo, 24
Rice, Donald, 17
Rinne, Yvonne, 2
Roach, Katherine, 4
Robles, Eva, 26
Roddy, Patrick, 10
Rodrigues, Fabiano, 12

Sadler, Brent, 33
Saito, Akinori, 18
Seemala, Gopi, 21
Seker, Ilgin, 28
Shi, Yong, 6
Spaletta, Jeffrey, 11
Stephan, Andrew, 14
Stoneback, Russell, 6
Stromberg, Erik, 33
Su, Yi-Jiun, 20
Sugar, Glenn, 25
Sunderland, Matthew, 14
Suresh, Padmashri, 15

Tambouret, Yann, 20
Thompson, Jonathan, 29
Twork, Gregory, 29

Urco Cordero, Juan, 17

Watts, Christopher, 16

Yin, Yan, 31

Yokoyama, Tatsuhiro, 29

Yonker, Justin, 5

Zettergren, Matthew, 31

Zhang, Lei, 10

Zhao, Siming, 15